Targeting ALK2: An Open Science Approach to Developing Therapeutics for the Treatment of Diffuse Intrinsic Pontine Glioma

Deeba Ensan,[†,§] *David Smil,*[§] *Carlos A. Zepeda-Velázquez,*[§] *Dimitrios Panagopoulos,*[§,Ↄ,ϰ] *Jong Fu Wong,*[‡] *Eleanor P. Williams,*[‡] *Roslin Adamson,*[‡] *Alex N. Bullock,*[‡] *Taira Kiyota,*[§] *Ahmed Aman,*[§,ζ] *Owen G. Roberts,*[ŧt] *Aled M. Edwards,*[ŧt,Ↄ] *Jeff A. O'Meara,*[§,ǂ] *Methvin B. Isaac,*[§] *Rima Al-awar*[*,§,†]

[†] Department of Pharmacology and Toxicology, University of Toronto, Medical Sciences Building, Room 4207, 1 King's College Circle, Toronto, Ontario M5S 1A8, Canada

[§] Drug Discovery Program, Ontario Institute for Cancer Research, 661 University Avenue, MaRS Centre, West Tower, Toronto, Ontario M5G 0A3, Canada

[Ↄ] Structural Genomics Consortium, University of Toronto, 101 College Street, MaRS Centre, South Tower, Toronto, Ontario M5G 1L7, Canada

[ϰ] Department of Chemistry, Simon Fraser University, 8888 University Drive, Burnaby, British Columbia V5A 1S6, Canada

‡ Structural Genomics Consortium, University of Oxford, Old Road Campus, Roosevelt Drive, Oxford OX3 7DQ, United Kingdom

ζ Leslie Dan Faculty of Pharmacy, University of Toronto, 144 College Street, Toronto, Ontario M5S 3M2, Canada

ᵗᵗ M4K Pharma Inc., 101 College Street, MaRS Centre, South Tower, Toronto, Ontario M5G 1L7, Canada

ABSTRACT

Diffuse intrinsic pontine glioma is an aggressive pediatric cancer for which no effective chemotherapeutic drugs exist. Analysis of the genomic landscape of this disease has led to the identification of the serine/threonine kinase ALK2 as a potential target for therapeutic intervention. In this work, we adopted an open science approach to develop a series of potent type I inhibitors of ALK2 which are orally bio-available and brain penetrant. Initial efforts resulted in the discovery of **M4K2009**, an analogue of the previously reported ALK2 inhibitor **LDN-214117**. Although highly selective for ALK2 over the TGF-βR1 receptor ALK5, **M4K2009** is also moderately active against the hERG potassium channel. Varying the substituents of the trimethoxyphenyl moiety gave rise to an equipotent benzamide analogue **M4K2149** with reduced off-target affinity for the ion channel. Additional modifications yielded 2-fluoro-6-methoxybenzamide derivatives (**26a-c**), which possess high inhibitory activity against ALK2, excellent selectivity and superior pharmacokinetic profiles.

INTRODUCTION

The design and development of brain penetrant kinase inhibitors as a therapy for the treatment of primary central nervous system (CNS) tumors entail numerous challenges. This is in part due to the remarkably different structural properties that CNS drugs and kinase inhibitors have.[1] Approved CNS drugs, for instance, have fewer hydrogen bond donors (HBDs), lower molecular weights and half the topological polar surface area (tPSA) of kinase inhibitors on average.[1] Elevated expression levels of efflux transporters at the blood-brain-barrier (BBB) constitute an additional obstacle that drugs must overcome in order to reach therapeutically relevant concentrations at sites of lesion. CNS drug exposure is further limited by the endothelial tight junctions of the BBB, which impede paracellular transport.[2] Despite these difficulties, the recent approval of Lorlatinib by the FDA for the treatment of metastatic anaplastic lymphoma kinase-positive non-small cell lung cancer demonstrates that the development of BBB penetrant kinase inhibitors is possible. There are multiple kinases in addition to the anaplastic lymphoma kinase that play pivotal roles in oncogenesis. Of interest to us are proteins involved in the bone morphogenetic protein (BMP) signaling pathway.

BMPs are a group of cytokines that modulate a plethora of physiological processes, including musculoskeletal development and neural differentiation.[3] The signal elicited by BMP binding to type II BMP receptors is transduced by type I BMP receptors, which promote the translocation of downstream effector proteins (SMADs) to the nucleus where they can regulate the transcription of target genes via chromatin remodeling.[4,5] Aberrant BMP signaling is implicated in a number of diseases,[5] such as fibrodysplasia ossificans progressiva (FOP). Germline mutations (c.617G>A; p.R206H) in the juxtamembrane glycine-serine (GS) rich domain of activin receptor-like kinase-2 (ALK2) confer gain of function activity to the type I BMP receptor and

contribute to the abnormal skeletal phenotype observed in individuals affected by FOP.[3,6] Somatic missense mutations in the *ACVR1* gene encoding ALK2 have also been reported in approximately 24% of children with the rare pediatric disease diffuse intrinsic pontine glioma (DIPG), with a higher prevalence of mutation occurring in the serine/threonine kinase domain of the receptor.[3,7]

DIPG is a grade IV tumor originating in the glial tissue of the pons.[3,7] Children affected by the disease have a 5-year relative survival rate of less than 1%.[8] Treatment options are limited to focal radiation therapy because of the sensitive area in which the tumor resides and the failure of currently available chemotherapeutic drugs to prolong survival.[8,9] The mechanism by which ALK2 contributes to DIPG pathogenesis has not yet been elucidated.[3,7,10] However, a recent study by Carvalho and co-workers demonstrated that shRNA knockdown of *ACVR1* elicits apoptosis in HSJD-DIPG-007 cells harboring *ACVR1* R206H mutations in conjunction with histone H3.3 K27M mutations.[11] Their work suggests that DIPG cells are dependent on enhanced BMP signaling. This was further recapitulated in their orthotopic patient-derived xenograft model in which administration of two ALK2 inhibitors extended survival compared to controls.[11] Although targeting the serine/threonine kinase may constitute a viable treatment, monotherapies are seldom efficacious for DIPG.[12] Targeting proteins with the potential to restore normal signatures, such as histone deacetylase (HDAC), has gained momentum in recent years.[12] It is likely that the most beneficial treatment option for patients will consist of combinatorial therapies.

Several inhibitors of ALK2 have emerged in the past decade,[13] including the pyrazolo[1,5-α]pyrimidine compound **LDN-193189**,[14-15] as well as a relatively new class of 3,5-diarylpyridine

analogues: **K02288**, **LDN-213844** and **LDN-214117**.[16-18] The triazolamine, CP466722, represents another novel chemotype with moderate binding affinity for ALK2 and unparalleled selectivity over other proteins in the serine/threonine kinase receptor (STKR) family.[19] Structure-activity relationship (SAR) studies surrounding this new scaffold should also be explored. As **LDN-214117** has been reported to have low cytotoxic activity and excellent kinome-wide selectivity,[17] we sought to explore whether additional modifications to the hinge-binding pyridyl core could improve ALK2 potency and selectivity over the closely related TGF-βRI receptor ALK5. Cardiotoxicity and gastrointestinal inflammation are adverse effects of ALK5 inhibition.[20] Therefore, a major focus of our SAR studies was to synthesize analogues with reduced off-target affinity for this receptor. Shifting the methyl substituent from the C-2 position of the pyridyl core of **LDN-214117** to the C-4 position (**M4K2009**), maintained potency and selectivity as determined by the *in vitro* and cell-based assays employed throughout our study (Figure 1).[21]

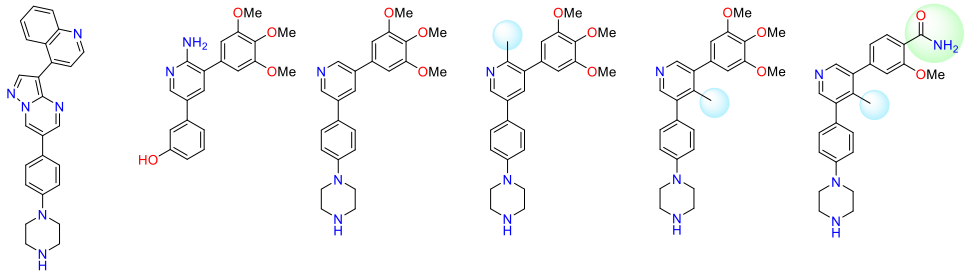

ALK2 Inhibitor		LDN-193189	K02288	LDN-213844	LDN-214117	M4K2009	M4K2149
ALK2 IC_{50} (nM)	**Reported**	0.7	35	15	24	-	-
	Measured	17	-	18	115	13	17
ALK5 IC_{50} (nM)	**Reported**	117	280	240	3000	-	-
	Measured	468	-	747	>2000	1830	576
Fold selectivity (ALK5/ALK2)	**Reported**	167	8	16	125	-	-
	Measured	28	-	42	>17	141	34

Figure 1: Inhibitory and off-target activity of previously reported ALK2 inhibitors and novel analogues. Reported values were obtained from the corresponding references.[15,17,18] Measured values were determined utilizing a radioactive biochemical kinase assay.

Although **M4K2009** has good structural and physicochemical properties, it poses the risk of eliciting torsades de pointes arrythmia *in vivo* due to the moderate affinity it has for the protein product encoded by the human ether-a-go-go related gene (hERG) (IC_{50} = 8 μM).[21] Additional modifications made to the trimethoxyphenyl moiety led to the identification of the benzamide analog **M4K2149**, which has a hERG IC_{50} of >50 μM and comparable inhibitory activity against ALK2 (Figure 1). In our pursuit of a potent, selective, orally bioavailable and brain penetrant type I inhibitor of ALK2, **M4K2149** was an excellent starting point from which to expand our SAR studies.

Our initial work with **M4K2009** revealed that the inhibitor was equipotent against both wild-type (WT) and mutant ALK2 (G328V, R206H and R258G) in the biochemical kinase assay.[21] These results are in alignment with the data generated by Mohedas and co-workers.[17] Utilizing a thermal shift kinase assay, they were able to demonstrate that FOP-causing mutations in both the GS and serine/threonine kinase domain of ALK2 had negligible effects on the kinase's affinity for type I inhibitors.[17] As FOP and DIPG patients harbor very similar mutations in the *ACVR1* gene,[3] the inhibitory activity of the compounds in our series was determined primarily against WT ALK2.

The potency and selectivity of our analogues was assessed using a radioactive *in vitro* kinase assay, employing **LDN-193189** as a control. To test the activity of the compounds in cells, a HEK293 cell-based NanoBRET assay from Promega was used. In this assay, the competitive displacement of a fluorescent tracer (PBI-6908) from the binding pocket of ALK2 by test compounds elicits reductions in BRET ratios, which are used to generate IC_{50} values. Cell-based potency against ALK5 was subsequently determined using a dual luciferase assay (DLA) in HEK293 cells.

The biological evaluation of these compounds was made possible by the *pro bono* contributions of Reaction Biology Corporation. This work, which was initiated by the open science pharmaceutical company M4K Pharma Inc., was performed in collaboration with the not-for-profit organizations, the Ontario Institute for Cancer Research (OICR) and the Structural Genomics Consortium (SGC). Adopting an open science approach enabled us to freely share and discuss results with experts in the field, forging collaborations that advanced the science without the delays associated with confidentiality agreements and intellectual property ownership.[22]

RESULTS AND DISCUSSION

Synthesis of Analogues

The synthetic route employed to prepare **M4K2149** and related analogues ultimately depended on the commercial availability of starting materials, ease of synthesis and reaction efficiency. The compounds were initially accessed as depicted in Scheme 1. Suzuki-Miyaura coupling of

3,5-dibromo-4-methylpyridine (**2**) with **1** generated intermediate **3**, which subsequently underwent Miyaura borylation to yield the boronate ester **4a**. Aromatic methyl esters **5a-b** were coupled with **4a** to afford intermediates **6a-b**, which were transformed to the corresponding primary amides **7a-b** by refluxing in methanolic ammonia, which was then followed by the removal of the carbamate protecting groups with trifluoroacetic acid (TFA). The preparation of analogues **8a-c** followed a similar synthetic route in which **4a** was coupled with the aromatic amides **5c-e** and then deprotected with TFA. Approximately 50% of intermediate **3** was converted to the undesired dehalogenated side-product **4b** in step *b*, which contributed to significantly low yields for the final products.

To overcome yield constraints, a second synthetic scheme was devised in which a wide variety of boronate esters were coupled with the pyridyl derivatives **3**, **10** or **15** (Scheme 2). The synthesis of the carboxylic acid intermediates **13a-b** was accomplished via a two-step, one-pot Suzuki-Miyaura coupling sequence. HATU-mediated coupling with ammonium chloride followed by deprotection, furnished the final amide regioisomers **14a-b**.

Scheme 1. Synthesis of Compounds **7a-b** and **8a-c**[a]

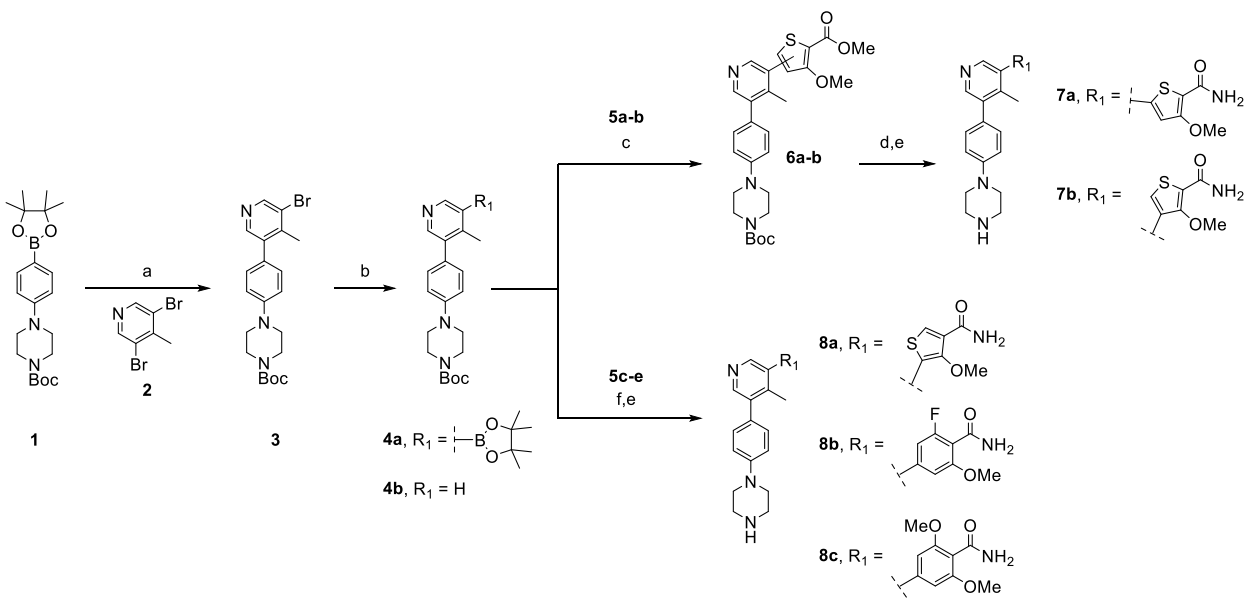

[a]Reagents and conditions: (a) $Pd(dppf)Cl_2 \cdot DCM$, Na_2CO_3, dioxane/H_2O, 85 ºC, overnight; (b) B_2pin_2, $Pd(dppf)Cl_2 \cdot DCM$, KOAc, dioxane, 110 ºC, 4 h; (c) aryl halide (**5a-b**), $Pd(dppf)Cl_2 \cdot DCM$, Na_2CO_3, dioxane/H_2O, 100 ºC, 2 h; (d) 7 N NH_3 in MeOH, 90 ºC, 3 d; (e) TFA, DCM, rt, overnight; (f) aryl halide (**5c-e**), XPhos Pd G2, K_3PO_4, dioxane/H_2O, 100 ºC, 3 h.

Suzuki-Miyaura coupling of **15** with the boronate ester **16** afforded the methyl ester intermediate **17**, which was converted to the corresponding primary, secondary or tertiary amide via aminolysis or base-catalyzed hydrolysis followed by EDC-mediated coupling with the desired amine. Deprotection using TFA or HCl afforded the compounds **M4K2149** and **18a-b**. A similar synthetic route was used to access analogues **20a-e**, although additional transformations beyond the standard Suzuki-Miyaura coupling and deprotection were not required, as the boronate esters **19a-e** already had the desired amide substituents installed.

Scheme 2. Synthesis of Compounds **14a-b**, **M4K2149**, **18a-b** and **20a-e**[a]

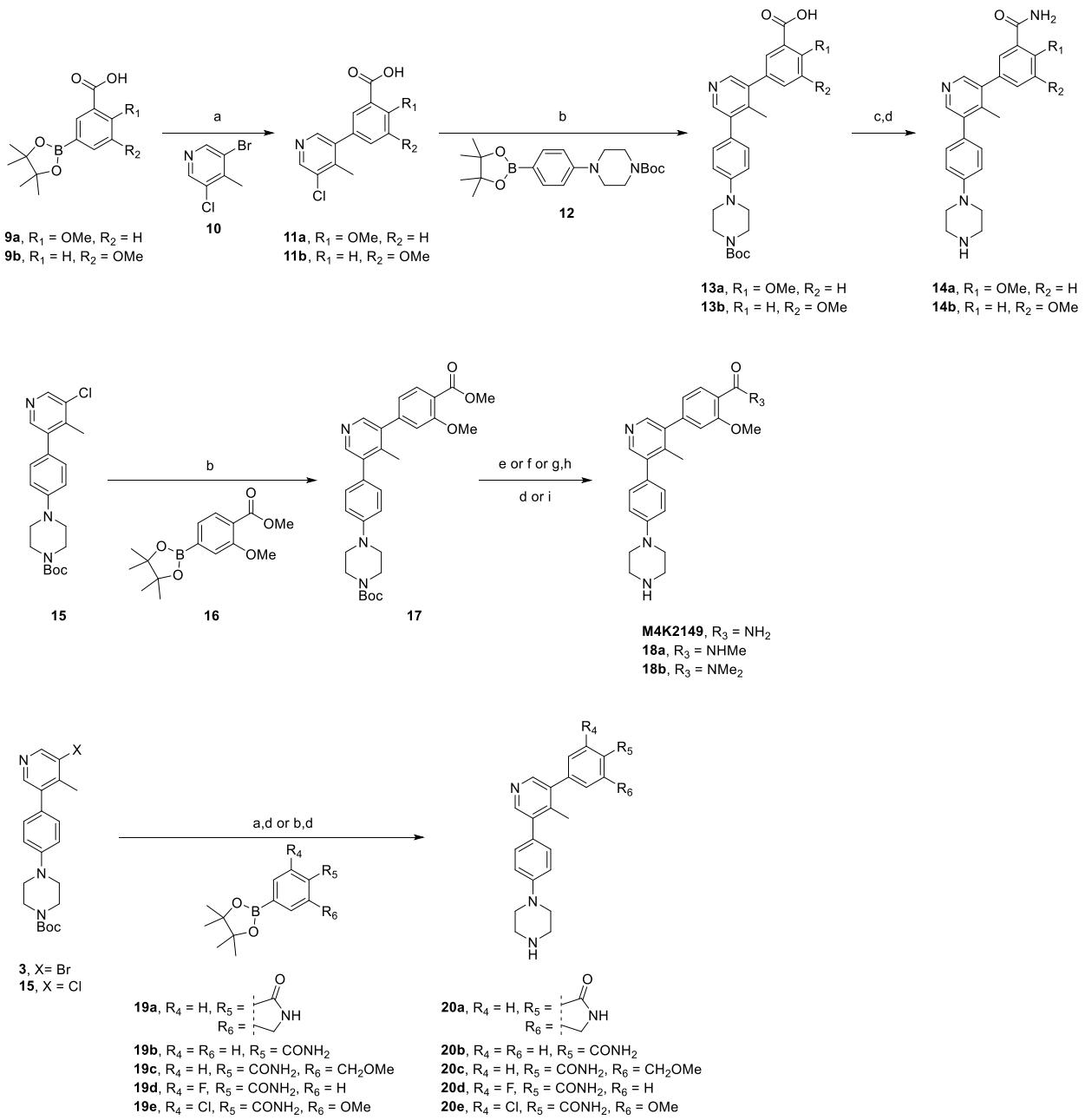

[a]Reagents and conditions: (a) $Pd(dppf)Cl_2 \cdot DCM$, Na_2CO_3, dioxane/H_2O, 100 ºC, 3 h; (b) XPhos Pd G2, K_3PO_4, dioxane/H_2O, 100 ºC, 3 h; (c) NH_4Cl, HATU, DIPEA, DCM, rt, 3 h; (d) TFA, DCM, rt, 1 h; (e) 7 N NH_3 in MeOH, 75 ºC, 3 d; (f) methylamine, MeOH, 85 ºC, 5 h; (g) KOH, THF/H_2O, rt, 2 h; (h) dimethylamine, HOBt, EDC, DIPEA, DCM/DMF, 50 ºC, overnight; (i) 4 M HCl in dioxane, MeOH, rt, 30 min.

The synthesis of analogues **26a-f** (Scheme 3) was initiated by the nucleophilic aromatic substitution of 4-bromo-2,6-difluorobenzonitrile (**21**) with sodium methoxide to yield both 4-bromo-2-fluoro-6-methoxybenzonitrile (**22a**) and 2,6-dimethoxybenzonitrile (**22b**). Both intermediates were hydrolyzed to the corresponding amides **5d-e** using hydrogen peroxide and an aqueous solution of sodium hydroxide. Miyaura borylation of **5d-e** followed by Suzuki-Miyaura coupling with 3-bromo-5-chloro-4-methylpyridine (**10**) afforded **24a-b**, which were subjected to a second coupling reaction with a variety of (4-(piperazin-1-yl)phenyl)boronate ester derivatives (**25a-c**) to furnish the final compounds **26a-f** in excellent yields.

Scheme 3: Synthesis of Compounds **26a-f**[a]

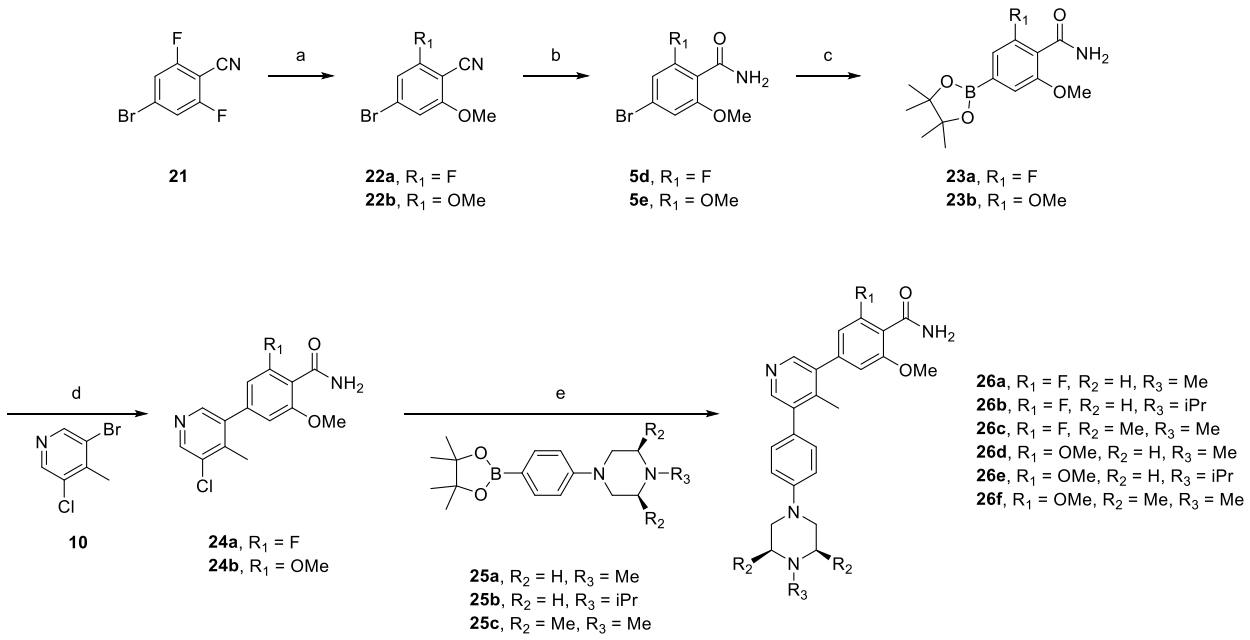

[a]Reagents and conditions: (a) NaH, MeOH, dioxane, rt, overnight; (b) H_2O_2, NaOH, EtOH/H_2O, overnight; (c) B_2pin_2, Pd(dppf)Cl_2·DCM, KOAc, dioxane, 110 ºC, 4 h; (d) Pd(dppf)Cl_2·DCM, Na_2CO_3, dioxane/H_2O, 100 ºC, 3 h; (e) XPhos Pd G2, K_3PO_4, dioxane/H_2O, 100 ºC, 3 h.

Structure Activity Relationship Studies

It has been disclosed by Mohedas and co-workers that the pyridyl nitrogen of **LDN-213844** participates in a key hydrogen bond interaction with the backbone amide of H286 in the hinge region of ALK2 (Figure 2B).[17] Our own crystallographic efforts led to the generation of a co-crystal structure of **M4K2149** with the kinase in high resolution, which revealed that the same interaction had been preserved (PDB code 6T6D). Furthermore, the trimethoxyphenyl motif of **LDN-213844** was reported to occupy a hydrophobic pocket of ALK2, where the *meta*-methoxy group participates in a water-mediated hydrogen bond with K235 (PDB code 4BGG).[17]

Substitution of the *para*-methoxy group of **LDN-213844** with a primary amide results in the establishment of a direct hydrogen bond between the carbonyl O of the amide and the NH_3^+ group of K235 (Figure 2A). Additionally, the phenyl ring of **M4K2149** stacks between G289 and V214,[23] while the protonated piperazine NH_2^+ is in close proximity to D293. This is suggestive of an electrostatic interaction. An intramolecular hydrogen bond between the amide NH_2 and O of the *ortho*-methoxy substituent can also be observed in the co-crystal structure.

A **B**

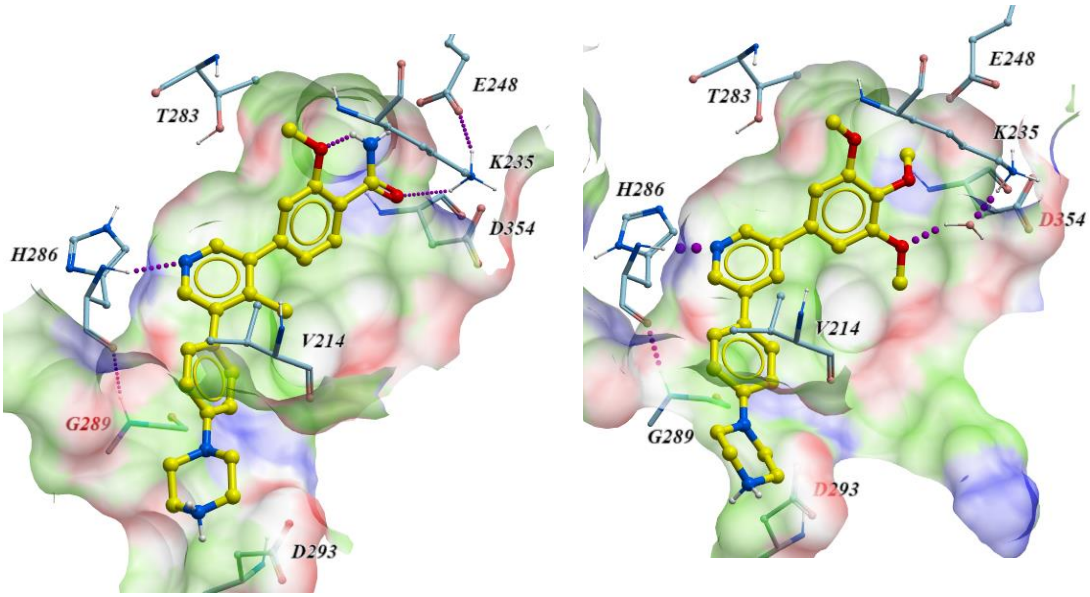

Figure 2. (A) Co-crystal structure of **M4K2149** (light yellow) with ALK2 (PDB code 6T6D). Hydrogen bonds are established with H286 and K235. The benzamide moiety of **M4K2149** occupies a hydrophobic pocket (green) of ALK2 and is flanked by several hydrogen bond donating (blue; K235) and hydrogen bond accepting residues (red; D354 and E248). The protonated piperazine motif is in close proximity to D293, indicative of an electrostatic interaction. (B) Co-crystal structure of **LDN-213844** (light yellow) with ALK2 (PDB code 4BGG). **M4K2149** and **LDN-213844** have similar modes of binding.

Our initial SAR studies focused on varying the substitution pattern of the amide in order to determine if the group could interact with other residues in the pocket, such as D354 of the DLG motif or E248.[23] Inverting the amide and methoxy substituents (**14a**) resulted in a complete loss of activity against ALK2 in the biochemical kinase assay. This correlated well with the results obtained by NanoBRET and DLA (Table 1). Moving the methoxy group from an *ortho*- to a *meta*-position with respect to the amide (**14b**) improved the biochemical potency compared to **14a**, however this did not translate into a significant improvement in cell-based potency. Replacement of the phenyl ring with 5-membered heterocycles gave rise to the thiophene analogues **7a-b** and **8a**, which were profiled to further investigate the effect that amide geometry had on potency and selectivity. A greater than 40-fold decrease in inhibitory activity against ALK2 was measured for **7a** and **7b**, while **8a** was found to be completely inactive against the kinase in both assays. It became evident that positioning the primary amide on a six-membered aromatic ring *para* to the hinge-binding pyridyl core was critical for maintaining key binding interactions with ALK2.

The consideration of several physicochemical parameters, such as lipophilicity (cLogP), tPSA and number of HBD is pertinent in the design of small molecule inhibitors that must penetrate the BBB to exert their pharmacological effects. The ideal values that brain penetrant drugs should have vary between reviews.[24] In the case of lipophilicity, the consensus is that immoderate increases in cLogP should be avoided. Although increasing the lipophilicity of a drug typically enhances potency and permeability, concomitant increases in nonspecific tissue binding also occur, which would ultimately decrease the concentration of free drug at its intended site of action within the brain.[24] The number of HBD that a molecule possesses, in addition to its tPSA, can also influence its ability to permeate the BBB. Increasing the value of

either physicochemical parameter also risks recognition by efflux transporters, such as P-glycoprotein (P-gp).[1,2]

Table 1: Inhibitory and off-target activities of **14a-b**, **7a-b** and **8a**

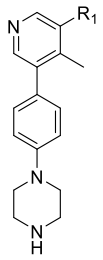

Compound	R_1	ALK2 IC_{50} (nM)	ALK5 IC_{50} (nM)	Fold Selectivity	NanoBRET ALK2 IC_{50} (nM)	DLA ALK5 IC_{50} (nM)	Cell-based Fold Selectivity
M4K2149	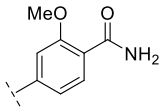	17	576	34	55[a]	704[b]	13
14a	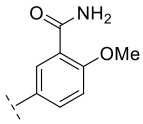	>1000	>5000	-	694	>5000	>7
14b	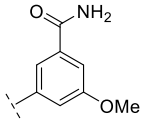	102	>5000	>49	588	>5000	>8
7a	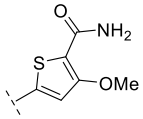	751	>5000	>6	3371	>5000	>1
7b	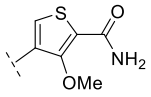	712	>5000	>7	2811	>5000	>1
8a	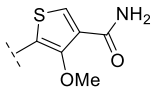	>1000	>5000	-	>5000	>5000	-

[a]Average of duplicate measurements. [b]Average of triplicate measurements.

With these guidelines in mind, we sought to determine if mono- and di-*N*-methylation of the primary amide, as well as its cyclization to form the corresponding isoindolinone analogue, could be tolerated. The effects of these modifications were two-fold. In addition to decreasing the number of HBD, the tPSA was reduced to below 70 $Å^2$ for **18a-b** and **20a**,[25] which is in an optimal range for CNS-penetrant drugs.[24] These structural changes had only moderate effects on the lipophilicity of the three analogues. Unfortunately, these compounds were discovered to be completely inactive against ALK2 (Table 2), indicating that the binding affinity of the benzamides may be sensitive to steric effects. Consequently, we decided to incorporate only the primary amide motif in the rest of our analogues.

To determine if the methoxy group of **M4K2149** was critical for maintaining potency, compound **20b** was profiled. Removal of the methoxy substituent reduced inhibitory activity against ALK2 by 28-fold. This result lead us to suspect that the methoxy group oriented the amide into a conformation that was ideal for ALK2 binding. The incorporation of intramolecular hydrogen bonds and electrostatic interactions to mask HBD is a technique commonly employed to enhance brain penetration.[1,24,26-28] In an attempt to exploit these interactions and probe for additional ones in the vicinity of the benzamide ring, we profiled compounds **20c** and **20d**, which featured a one-carbon homologation of the methoxy group and a bioisosteric replacement of the methoxy for a fluorine atom, respectively. Both modifications, however, failed to improve biochemical potency against ALK2.

Table 2: Inhibitory and off-target activities of **8b-c**, **18a-b**, **20a-e**

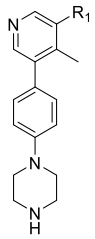

Compound	R_1	ALK2 IC_{50} (nM)	ALK5 IC_{50} (nM)	Fold Selectivity	NanoBRET ALK2 IC_{50} (nM)	DLA ALK5 IC_{50} (nM)	Cell-based Fold Selectivity
M4K2149	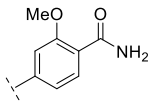	17	576	34	55[a]	704[b]	13
18a	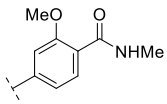	>1000	>5000	-	>5000	>5000	-
18b	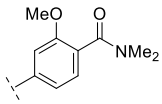	>1000	>5000	-	>5000	>5000	-
20a	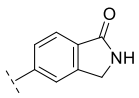	652	>5000	>7	2336	4810	2
20b	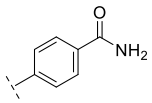	477	>5000	>10	2771	>5000	>1
20c	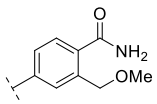	687	>5000	>7	3845	>5000	>1
20d	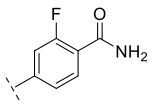	263	>5000	>19	1013	>5000	>4
8b	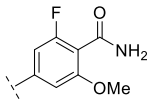	24	1920	80	81	3554	44
20e	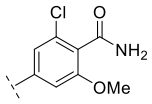	9	2080	231	93	>5000[a]	>54
8c	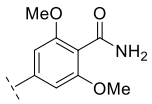	5	46	9	178	216	1

[a]Average of duplicate measurements. [b]Average of triplicate measurements.

Incorporation of both a fluorine and methoxy substituent *ortho* to the amide gave rise to compound **8b**, which not only had a biochemical ALK2 potency comparable to that of **M4K2149** (ALK2 IC_{50} = 24 nM), but also an improved selectivity profile over ALK5. These results correlated well with those obtained in the NanoBRET and DLA assays (Table 2). Exactly how the fluorine substituent contributes to this enhancement in selectivity is yet to be elucidated, although two possible explanations exist. We surmised that the electron-withdrawing nature of the fluorine atom decreases the ability of the carbonyl O to act as a hydrogen bond acceptor,[28] thereby reducing the strength of intermolecular interactions that may be more critical for ligand binding to ALK5 than ALK2. The second possible explanation focuses on how the halogen substituent affects the conformation of the amide with respect to the phenyl ring. For anisole and benzamide motifs, which typically adopt planar topologies, *ortho* substituents can force the methoxy or amide groups out of the plane of the benzene ring in order to reduce allylic strain.[28-29] We postulated that a similar phenomenon could be occurring in the case of **8b** and that this change in conformation is better tolerated by ALK2 than ALK5.

We decided to introduce a larger substituent *ortho* to the amide in order to confirm whether the latter hypothesis was correct. Replacing the fluorine atom of **8b** with a chlorine atom (**20e**) increased the biochemical selectivity over ALK5 to greater than 200-fold, suggesting that our proposed explanation is a reasonable one. However, NanoBRET ALK2 IC_{50} values were similar for both **8b** and **20e**, indicating that the modification has little impact on ALK2 potency. To determine if electron-donating groups could be tolerated at this position as well, **8c** was prepared.

This analogue had the greatest structural similarity to our lead compound **M4K2009**. Although **8c** was the most potent analogue in our series, it suffered from poor selectivity (biochemical selectivity of 9-fold over ALK5). Additionally, there was a substantial difference in its biochemical and cell-based potencies (biochemical ALK2 IC_{50} = 5 nM vs NanoBRET ALK2 IC_{50} = 178 nM).

Table 3: Inhibitory and off-target activity of 2-fluoro-6-methoxybenzamide and 2,6-dimethoxybenzamide analogues, **26a-f**

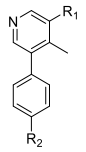

Compound	R_1	R_2	ALK2 IC_{50} (nM)	ALK5 IC_{50} (nM)	Fold Selectivity	NanoBRET ALK2 IC_{50} (nM)	DLA ALK5 IC_{50} (nM)	Cell-based Fold Selectivity
8b	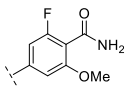		24	1920	80	81	3554	44
26a	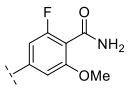		3	1050	350	93	4297[a]	46
26b	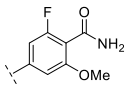	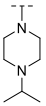	5[a]	2144[a]	429	52	3900[a]	75
26c	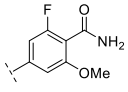		10	2910	291	100	>5000[a]	>50
8c	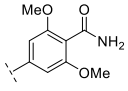		5	46	9	178	216	1
26d	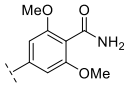		<3[b]	75[b]	-	19[c]	249[d]	13
26e	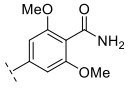	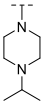	5	66	13	18	276[a]	15
26f	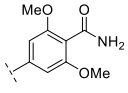		3	52	17	21	283[a]	13

[a]Average of duplicate measurements. [b]Average of triplicate measurements. [c]Average of quadruplicate measurements. [d] Average of quintuplicate measurements.

Permeability, Selectivity and Pharmacokinetic Studies

Having identified several potent analogues, we decided to focus our efforts on improving the pharmacokinetic (PK) profiles of two; **8b** and **8c**. In order to assess the permeability of these compounds, they were tested in a Caco-2 assay, which revealed that both analogues were poorly permeable and being recognized by efflux transporters (efflux ratios for both **8b** and **8c** were >30) (see Table 4 and Table 2 in Supporting Information). In an attempt to reduce efflux, the terminal piperazine nitrogens of **8b** and **8c** were capped with various alkyl groups to generate 1-methyl-, 1-isopropyl- and 1,2,6-trimethylpiperazine analogs (**26a-f**).[30] In addition to reducing the number of HBD, methylation of the terminal piperazine nitrogen offered the additional advantage of attenuating pKa,[25,31] which is often associated with a decrease in P-gp-mediated efflux.[24] The rationale behind incorporating methyl groups at positions 1, 2 and 6 of the piperazine groups was to increase the molecular rigidity of analogues **26c** and **26f**. This is a strategy that is commonly employed to enhance brain penetration and oral bioavailability.[24] As it has been reported that the piperazine motif of **LDN-193189** is a metabolic liability,[32] increasing the steric bulk around this group was also done to improve the inhibitors' ADME profile *in vivo*.

As anticipated, the permeability (P_{app_AB}) of the 2-fluoro-6-methoxybenzamide analogues was increased from 0.3 x 10^{-6} cm/s (**8b**) to around 5.0 x 10^{-6} cm/s for **26a-c**. This was accompanied by a concomitant reduction in the efflux ratio (from >30 for **8b** to less than 3.0 for **26a** and **26b**) (Table 4). An enhancement in selectivity over ALK5 was also observed for these compounds. This was more pronounced in the biochemical kinase assay (Table 3). Unfortunately, similar results were not obtained for the 2,6-dimethoxybenzamide analogues (**26d-f**). Piperazine

alkylation appeared to have little effect on reducing efflux (see Supporting Information, Table 2). However, **26d-f** demonstrated excellent inhibitory activity against ALK2 in the NanoBRET assay. Although **M4K2149** and **8c** differ by only one methoxy group, the latter analogue had a significantly higher efflux ratio (8.1 vs >30).[21] We suspected that the extra electron-donating group was increasing the hydrogen bond acceptor potential of the amide carbonyl, which was being recognized by one of the efflux transporters expressed by the Caco-2 cells. Consequently, these analogues were excluded from further profiling.

Prior to assessing the PK profiles of the 2-fluoro-6-methoxybenzamide analogues *in vivo*, the metabolic stabilities of **8b** and **26a-c** were evaluated in mouse and human liver microsomal (MLM and HLM) stability assays. All four analogues exhibited moderate to high stability in both *in vitro* assays, with compounds **8b** and **26b** demonstrating the highest degree of stability after a 60-minute incubation period at 37 ºC (>85% remaining) (see the Supporting Information, Table 3). Oral administration of a 10 mg/kg dose of **8b** in female CB17 SCID mice (n = 3) gave rise to suboptimal values for C_{max} (97 ng/mL), $t_{1/2}$ (1.31 h) and AUC_{inf} (296 ng·h/mL). Given the poor intrinsic permeability of **8b**, these results were not surprising. A significant improvement in PK properties was observed for analogs **26a** and **26b**, both of which yielded a greater than 17-fold increase in C_{max}, 13-fold increase in AUC_{inf} and a doubling of $t_{1/2}$ (Table 4). The two analogues were also assessed for their ability to penetrate the BBB in the same strain of mice. Oral administration of these compounds at a 100 mg/kg dose gave rise to average total brain concentrations of 777 and 1595 ng/g and total brain-to-plasma ratios (*B/P*) of 0.178 and 0.132 for **26a** and **26b**, respectively. Although these values are moderate, the use of *B/P* ratios to assess brain permeability is generally not encouraged. The extent of brain penetration is

typically evaluated based on the ratio of the unbound brain concentration to the unbound plasma concentration ($K_{p,uu}$).[2] Whether these analogues require additional modifications to enhance BBB permeability will ultimately depend on the value of this parameter.

Table 4: *In vitro* permeability and oral *in vivo* PK studies of 2-fluoro-6-methoxybenzamide analogues

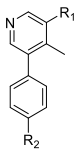

Compound	R_1	R_2	Caco-2 Permeability Assay			PK in Female SCID Mice (10 mg/kg PO dose) (n = 3)		
			P_{app_AB} (10^{-6} cm/s	P_{app_BA} (10^{-6} cm/s)	Efflux ratio	C_{max} (ng/mL)	AUC_{inf} (ng·h/mL)	$t_{1/2}$ (h)
8b	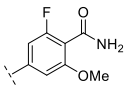		0.3	10.7	>30	97	296	1.31
26a	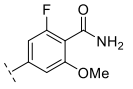		5.5	16.2	2.9	2140	4056	2.56
26b	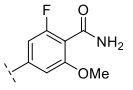	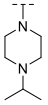	5.7	15.1	2.6	1650	4630	2.61
26c	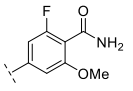		4.3	14.5	3.4	-	-	-

To ensure that a favorable hERG profile had been maintained for the 2-fluoro-6-methoxybenzamide analogues, their potencies against the hERG potassium channel were assessed using a HEK293 cell-based patch-clamp assay. **26a** and **26b** had optimal hERG IC_{50} values of >30 μM, while **26c** was slightly more potent against the ion channel (IC_{50} = 19 μM)

(see the Supporting Information, Table 4). To further investigate the off-target activity of these analogues, we profiled them in a 375-member kinase panel. At a concentration of 1 μM for each of the three compounds, fewer than 5% of the kinases showed a greater than 50% reduction in enzymatic activity. Excluding ALK1, 2, 3 and 6, the kinases ARAF, MAP4K4, MINK and TNK1 were the most sensitive to inhibition by **26a-c** (see Supporting Information, Table 5). We were also encouraged by the results obtained in an *in vitro* CYP inhibition assay, which showed that these analogues had negligible inhibitory activity (IC_{50} > 50 μM) against 7 CYP isoforms (CYP1A2, 2B6, 2C8, 2C9, 2C19, 2D6 and 3A4) (see Supporting Information, Table 4). Altogether, these results demonstrate that we were able to meet our objective of designing selective and orally bioavailable inhibitors of ALK2. Furthermore, profiling 7 analogues against 3 ALK2 mutants (R206H, G328V and R258G) in a radioactive *in vitro* kinase assay revealed that, similar to **M4K2009**, the analogues had comparable potencies against both WT and mutant ALK2 (Table 5). These findings confirm that the benzamide inhibitors developed in this series have the potential to regulate aberrant BMP signaling in patients harboring these mutations.

Table 5: Inhibitory activity of benzamide analogs against WT and DIPG-linked mutant forms of ALK2

Compound	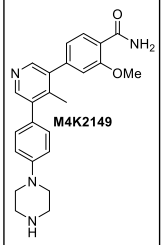 M4K2149	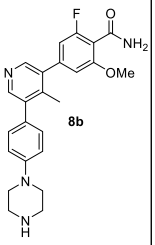 8b	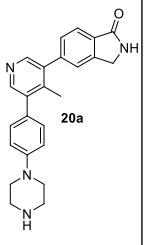 20a	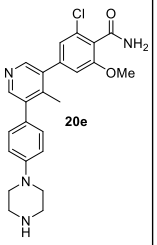 20e	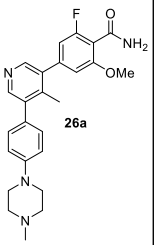 26a	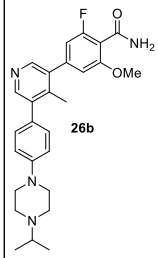 26b	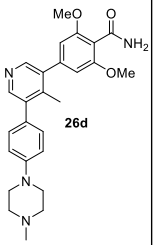 26d
ALK2 (WT) IC_{50} (nM)	17	24	652	9	3	5	<3
ALK2 (G328V) IC_{50} (nM)	5	4	171	<2	16	3	<2
ALK2 (R206H) IC_{50} (nM)	9	8	226	5	19	6	4
ALK2 (R258G) IC_{50} (nM)	9	7	363	4	17	6	<2

Conclusion

Advances in the development of effective chemotherapeutic agents for the treatment of DIPG have been limited. This is in part due to the convoluted genomic signatures of DIPG, which has made our understanding of its pathogenesis difficult. Recent identification of ALK2 as a target for therapeutic intervention has prompted the emergence of several classes of type I kinase inhibitors. In this work, we expanded the SAR of the 3,5-diarylpyridine inhibitor **LDN-214117**, which led to the discovery of a potent benzamide analogue **M4K2149** with an attenuated affinity for the hERG potassium channel. We determined that we could tailor the selectivity of our analogues over ALK5 by incorporating halogen substituents at a position *ortho* to the amide

group of **M4K2149**. We were also able to address issues of permeability by capping the NH of the solvent-exposed piperazine group. The resulting 2-fluoro-6-methoxybenzamide derivatives **26a-c** demonstrated excellent kinome-wide selectivity and had improved PK properties compared to their parent compound **8b**. Furthermore, the co-crystal structure of **M4K2149** with ALK2 helped us rationalize potency differences between analogues in the series and highlighted structural motifs that were crucial for maintaining key interactions with the protein. Despite these optimizations, total brain-to-plasma ratios are inadequate for accurately assessing the pharmacological activity of **26a-b** in the brain. Measuring the unbound brain concentrations ($C_{b,u}$) of these analogues *in vivo* is therefore warranted. These data would ultimately determine whether additional modifications should be made to reduce efflux/enhance permeability. Nonetheless, these benzamides represent a new chemotype possessing high inhibitory activity against both WT and mutant ALK2. Implementation of an open science model accelerated the development of these analogs by promoting communication between the chemists involved in their design and establishing a pipeline for rapidly generating biological data. Future work will continue to use open science to develop novel classes of ALK2 inhibitors. The analogues presented in this study have the potential to deepen our understanding of the biology of DIPG and will hopefully pave the way for future chemotherapies.

EXPERIMENTAL

Chemistry

All reagents were purchased from commercial vendors and used without further purification. Volatiles were removed under reduced pressure by rotary evaporation or by using the V-10 solvent evaporator system by Biotage®. Very high boiling point (6000 rpm, 0 mbar, 56 °C), mixed volatile

(7000 rpm, 30 mbar, 36 ºC) and volatile (6000 rpm, 30 mbar, 36 ºC) methods were used to evaporate solvents. The yields given refer to chromatographically purified and spectroscopically pure compounds. Compounds were purified using a Biotage Isolera One system by normal phase chromatography using Biotage® SNAP KP-Sil or Sfär Silica D columns (Part No.: FSKO-1107/FSRD-0445) or by reverse-phase chromatography using Biotage® SNAP KP-C18-HS or Sfär C18 D columnds (Part No.: FSLO-1118/FSUD-040). If additional purification was required, compounds were purified by solid phase extraction (SPE) using Biotage Isolute Flash SCX-2 cation exchange cartridges (Part No.: 532-0050-C and 456-0200-D). Products were washed with 2 cartridge volumes of MeOH and eluted with a solution of MeOH and NH_4OH (9:1 v/v). Preparative chromatography was carried out using a Waters 2767 injector with the collector attached to PDA UV/Vis and SQD mass detectors. An XSelect CSH Prep C18 5µm OBD 19 mm x 100 mm (Part No.: 186005421) or Xselect CSH Prep C18 5µm 10 mm x 100 mm (Part No.: 186005415) column was used for purification. Final compounds were dried using the Labconco™ Benchtop FreeZone™ Freeze-Dry System (4.5 L Model). ^{1}H and proton-decoupled ^{19}F NMRs were recorded on a Bruker Avance-III 500 MHz spectrometer at ambient temperature. Residual protons of $CDCl_3$, DMSO-d_6 and CD_3OD solvents were used as internal references. Spectral data are reported as follows: chemical shift (δ in ppm), multiplicity (br = broad, s = singlet, d = doublet, dd = doublet of doublets, m = multiplet), coupling constants (J in Hz) and proton integration. Compound purity was determined by UV absorbance at 254 nm during tandem liquid chromatography/mass spectrometry (LCMS) using a Waters Acquity separations module. **All final compounds had a purity of ≥95% as determined using this method.** Low resolution mass spectrometry (LRMS) was conducted in positive ion mode using a Waters Acquity SQD mass spectrometer (electrospray ionization source) fitted with a PDA detector. Mobile phase A

consisted of 0.1% formic acid in water, while mobile phase B consisted of 0.1% formic acid in acetonitrile. One of three types of columns were used: Column 1: Acquity UPLC CSH C18 (2.1 x 50 mm, 130 Å, 1.7 µm. Part No. 186005296), Column 2: Acquity UPLC BEH C8 (2.1 x 50 mm, 130 Å, 1.7 µm. Part No. 186002877) or Column 3: Acquity UPLC HSS T3 (2.1 x 50 mm, 100 Å, 1.8 µm. Part No. 186003538). For columns 1 and 2, the gradient went from 90% to 5% mobile phase A over 1.8 min, maintained at 5% for 0.5 min, then increased to 90% over 0.2 min for a total run time of 3 min. For column 3, the gradient went from 98% to 5% mobile phase A over 1.8 min, maintained at 5% for 0.5 min, then increased to 98% over 0.2 min for a total run time of 3 min, as well. The flow rate was 0.4 mL/min throughout both runs. All columns were used with the temperature maintained at 25 °C. High resolution mass spectrometry was conducted using a Waters Synapt G2-S quadrupole-time-of-flight (QTOF) hybrid mass spectrometer system coupled with an Acquity ultra-performance liquid chromatography (UPLC) system. Chromatographic separations were carried out on an Acquity UPLC CSH C18 (2.1 x 50 mm, 130 Å, 1.7 µm. Part No. 186005296), Acquity UPLC BEH C8 (2.1 x 50 mm, 130 Å, 1.7 µm. Part No. 186002877) or Acquity UPLC HSS T3 (2.1 x 50 mm, 100 Å, 1.8 µm. Part No. 186003538). The mobile phase was 0.1% formic acid in water (solvent A) and 0.1% formic acid in acetonitrile (solvent B). Leucine Enkephalin was used as lock mass. MassLynx 4.1 was used for data analysis.

Tert-butyl 4-(4-(5-bromo-4-methylpyridin-3-yl)phenyl)piperazine-1-carboxylate (3)

A solution of tert-butyl 4-[4-(4,4,5,5-tetramethyl-1,3,2-dioxaborolan-2-yl)phenyl]tetrahydro-1(2H)-pyrazinecarboxylate (**1**) (1.549 g, 3.99 mmol), 3,5-dibromo-4-methylpyridine (**2**) (0.953 g, 3.80 mmol), [1,12-bis(diphenylphosphino)ferrocene]dichloropalladium(II)·DCM complex (0.310 g, 0.38 mmol) and sodium carbonate monohydrate (1.414 g, 11.40 mmol) in 1,4-dioxane (16.3 mL) and water (2.7 mL) was heated to 85 °C and stirred overnight. The reaction mixture was

concentrated under reduced pressure prior to dilution with water (30 mL) and extraction with EtOAc (3 x 30 mL). The combined extracts were dried over $MgSO_4$ and concentrated to yield a brown oil. The crude material was purified by silica gel chromatography (0-50% EtOAc in hexanes) to afford a white solid (0.770 g, 47% yield). ^{1}H NMR (500 MHz, $CDCl_3$) δ 8.61 (s, 1H), 8.31 (s, 1H), 7.20 (d, *J* = 8.6 Hz, 2H), 6.99 (d, *J* = 8.8 Hz, 2H), 3.65 – 3.56 (m, 4H), 3.26 – 3.18 (m, 4H), 2.36 (s, 3H), 1.49 (s, 9H). MS (ESI): *m/z* = 432.31 $[M + H]^+$, 434.38 $[M + H]^+ + 2$.

(5-(4-(4-(Tert-butoxycarbonyl)piperazin-1-yl)phenyl)-4-methylpyridin-3-yl)boronic acid (4a)

A solution of **3** (171 mg, 0.396 mmol), bis(pinacolato)diboron (201 mg, 0.792 mmol), [1,12-bis(diphenylphosphino)ferrocene]dichloropalladium(II)·DCM complex (32 mg, 0.040 mmol) and potassium acetate (78 mg, 0.792 mmol) in 1,4-dioxane (4 mL) was microwaved at 110 °C for 4 h. The mixture was transferred to a 15 mL Falcon tube and centrifuged for 1 min at 4000 rpm. The dark brown supernatant was used without further purification in subsequent reactions (190 mg, 57% yield). MS (ESI): *m/z* = 397.90 $[M + H]^+$.

5-Chloro-4-methoxythiophene-3-carboxamide (5c)

The title compound was prepared using a modified literature procedure.[33] To a solution of 5-chloro-4-methoxythiophene-3-carboxylic acid (100.0 mg, 0.519 mmol) in DCM (1.5 mL) was added ammonium chloride (33.3 mg, 0.623 mmol), HATU (237.0 mg, 0.623 mmol) and DIPEA (271 µL, 1.558 mmol). The reaction mixture was stirred at room temperature for 3 h. Volatiles were removed under reduced pressure and the crude product was purified by silica gel chromatography (0-100% EtOAc in hexanes) to afford an off-white solid (71.1 mg, 72% yield). ^{1}H NMR (500 MHz, $CDCl_3$) δ 7.91 (s, 1H), 7.21 (br s, 1H), 5.72 (br s, 1H), 4.06 (s, 3H). MS (ESI): *m/z* = 192.27 $[M + H]^+$, 194.28 $[M + H]^+ + 2$.

4-Bromo-2-fluoro-6-methoxybenzamide (5d)

The title compound was prepared using modified literature procedures.[34-35] A solution of 4-bromo-2-fluoro-6-methoxybenzonitrile (**22a**) (5.00 g, 21.74 mmol) in EtOH (100.0 mL) was cooled in an ice bath prior to the addition of an aqueous solution of sodium hydroxide (0.43 M, 65.0 mL). This was followed by the addition of hydrogen peroxide (30 wt. % solution in water) (26.6 mL). The solution was stirred at room temperature overnight. The reaction mixture was concentrated under reduced pressure prior to dilution with water (250 mL) and extraction with EtOAc (3 x 250 mL). The combined organic extracts were dried over Na_2SO_4, filtered and concentrated under reduced pressure to give a white crystalline solid (4.63 g, 80% yield). ^{1}H NMR (500 MHz, DMSO) δ 7.84 (br s, 1H), 7.58 (br s, 1H), 7.17 (d, *J* = 8.5 Hz, 1H), 7.13 (s, 1H), 3.82 (s, 3H). ^{19}F NMR (471 MHz, DMSO) δ -115.38. MS (ESI): *m/z* = 248.20 $[M + H]^+$, 250.27 $[M + H]^+ + 2$.

4-Bromo-2,6-dimethoxybenzamide (5e)

The title compound was synthesized according to the procedure described for **5c** from 4-bromo-2,6-dimethoxybenzoic acid (157 mg, 0.600 mmol). The final product was a white solid (100 mg, 64% yield). ^{1}H NMR (500 MHz, DMSO) δ 7.51 (br s, 1H), 7.23 (br s, 1H), 6.87 (s, 2H), 3.75 (s, 6H). MS (ESI): *m/z* = 260.35 $[M + H]^+$, 262.29 $[M + H]^+ + 2$.

The title compound was alternatively synthesized according to the procedure described for **5d** from 4-bromo-2,6-dimethoxybenzonitrile (**22b**) (968 mg, 4.00 mmol), hydrogen peroxide (30 wt. % solution in water) (9.8 mL) and an aqueous solution of sodium hydroxide (2 M, 25.0 mL). The reaction mixture was heated to 110 °C for 8 h. The solvents were evaporated and the crude material was suspended in water, filtered and dried under high vacuum to afford a white crystalline solid (903 mg, 87% yield).

3-Methoxy-5-(4-methyl-5-(4-(piperazin-1-yl)phenyl)pyridin-3-yl)thiophene-2-carboxamide (6a)

A solution of **4a** (80 mg, 0.167 mmol), methyl 5-bromo-3-methoxythiophene-2-carboxylate (42 mg, 0.167 mmol) (**5a**), [1,12-bis(diphenylphosphino)ferrocene]dichloropalladium(II)·DCM complex (14 mg, 0.017 mmol) and sodium carbonate monohydrate (62 mg, 0.501 mmol) in 1,4-dioxane (2.9 mL) and water (477 µL) was heated to 100 ^{o}C for 2 h. The reaction mixture was adsorbed onto celite and the volatiles were removed under reduced pressure. The crude product was purified by silica gel chromatography (0-100% EtOAc in hexanes) to afford an off-white powder (45 mg, 50% yield). MS (ESI): *m/z* = 524.70 $[M + H]^{+}$.

Tert-butyl 4-(4-(5-(4-methoxy-5-(methoxycarbonyl)thiophen-3-yl)-4-methylpyridin-3-yl)phenyl)piperazine-1-carboxylate (6b)

The title compound was synthesized according to the procedure described for **6a** from **4a** (80 mg, 0.167 mmol) and methyl 4-bromo-3-methoxythiophene-2-carboxylate (**5b**) (42 mg, 0.167 mmol). The final product was a light yellow powder (47 mg, 52% yield). MS (ESI): *m/z* = 524.70 $[M + H]^{+}$.

3-Methoxy-5-(4-methyl-5-(4-(piperazin-1-yl)phenyl)pyridin-3-yl)thiophene-2-carboxamide (7a)

A 5 mL MW vial was charged with **6a** (20.0 mg, 0.038 mmol). The material was dissolved in a solution of ammonia in methanol (7N) (4 mL). The vial was sealed and the solution was stirred at 90 ^{o}C for 3 days. Volatiles were removed under reduced pressure and the crude material was purified by silica gel chromatography (0-100% EtOAc in hexanes). The purified product was dissolved in DCM (1 mL) and treated with trifluoroacetic acid (88 µL, 1.146 mmol). The

solution was stirred overnight. The product was purified by SPE. Drying under high vacuum overnight afforded an off-white powder (7.8 mg, 47% yield). ^{1}H NMR (500 MHz, DMSO) δ 8.37 (s, 1H), 8.36 (s, 1H), 7.76 (s, 1H), 7.66 (br s, 1H), 7.31 – 7.25 (m, 3H), 7.05 (d, *J* = 8.7 Hz, 2H), 3.51 (s, 3H), 3.22 – 3.20 (m, 4H), 2.98 – 2.94 (m, 4H), 2.13 (s, 3H). HRMS (ESI) for $C_{22}H_{24}N_4O_2S$ $[M + H]^+$: *m/z* = calcd, 409.1693; found, 409.1691.

3-Methoxy-4-(4-methyl-5-(4-(piperazin-1-yl)phenyl)pyridin-3-yl)thiophene-2-carboxamide (7b)

The title compound was synthesized according to the procedure described for **7a** from **6b** (20.0 mg, 0.038 mmol). The final product was an off-white powder (8.9 mg, 53% yield). ^{1}H NMR (500 MHz, DMSO) δ 8.38 (s, 1H), 8.36 (s, 1H), 7.76 (s, 1H), 7.66 (br s, 1H), 7.30 – 7.26 (m, 3H), 7.04 (d, *J* = 8.7 Hz, 2H), 3.52 (s, 3H), 3.19 – 3.17 (m, 4H), 2.95 – 2.91 (m, 4H), 2.13 (s, 3H). HRMS (ESI) for $C_{22}H_{24}N_4O_2S$ $[M + H]^+$: *m/z* = calcd, 409.1693; found, 409.1689.

4-Methoxy-5-(4-methyl-5-(4-(piperazin-1-yl)phenyl)pyridin-3-yl)thiophene-3-carboxamide (8a)

A solution of **4a** (60.0 mg, 0.125 mmol), **5c** (20.0 mg, 0.104 mmol), XPhos Pd G2 (8.2 mg, 0.010 mmol) and potassium phosphate tribasic (44.3 mg, 0.209 mmol) in 1,4-dioxane (1.8 mL) and water (298 µL) was heated to 100 ºC for 3 h. The reaction mixture was adsorbed onto celite and volatiles were removed under reduced pressure. The crude product was purified by silica gel chromatography (0-100% EtOAc in hexanes). Further purification was carried out by reverse-phase chromatography (2-95% ACN (0.1% formic acid) in water (0.1% formic acid)). The product was dissolved in DCM (1 mL) and treated with trifluoroacetic acid (479 µL, 6.26 mmol). The solution was stirred for one hour. The product was purified by SPE. Freeze drying for 3 days afforded an off-white powder (6.5 mg, 15% yield). ^{1}H NMR (500 MHz, DMSO) δ 8.44 (s,

1H), 8.39 (s, 1H), 8.11 (s, 1H), 7.47 (br s, 1H), 7.44 (br s, 1H), 7.30 (d, *J* = 8.5 Hz, 2H), 7.05 (d, *J* = 8.7 Hz, 2H), 3.57 (s, 3H), 3.24 – 3.21 (m, 4H), 3.01 – 2.96 (m, 4H), 2.17 (s, 3H). HRMS (ESI) for $C_{22}H_{24}N_4O_2S$ $[M + H]^+$: *m/z* = calcd, 409.1693; found, 409.1694.

2-Fluoro-6-methoxy-4-(4-methyl-5-(4-(piperazin-1-yl)phenyl)pyridin-3-yl)benzamide (8b)

The title compound was synthesized according to the procedure described for **8a** from **4a** (77 mg, 0.161 mmol) and **5d** (40 mg, 0.161 mmol). The final product was an off-white powder (20 mg, 29% yield). ^{1}H NMR (500 MHz, DMSO) δ 8.38 (s, 1H), 8.34 (s, 1H), 7.89 (br s, 1H), 7.58 (br s, 1H), 7.30 (d, *J* = 8.6 Hz, 2H), 7.04 (d, *J* = 8.6 Hz, 2H), 6.98 – 6.95 (m, 2H), 3.85 (s, 3H), 3.19 – 3.15 (m, 4H), 2.94 – 2.89 (m, 4H), 2.19 (s, 3H). ^{19}F NMR (471 MHz, DMSO) δ -116.73. HRMS (ESI) for $C_{24}H_{25}FN_4O_2$ $[M + H]^+$: *m/z* = calcd, 421.2034; found, 421.2040.

2,6-Dimethoxy-4-(4-methyl-5-(4-(piperazin-1-yl)phenyl)pyridin-3-yl)benzamide (8c)

The title compound was synthesized according to the procedure described for **8a** from **4a** (190 mg, 0.396 mmol) and **5e** (82 mg, 0.317 mmol). The final product was an off-white powder (45 mg, 32% yield). ^{1}H NMR (500 MHz, DMSO) δ 8.36 (s, 1H), 8.35 (s, 1H), 7.57 (br s, 1H), 7.31 (d, *J* = 8.6 Hz, 2H), 7.23 (br s, 1H), 7.04 (d, *J* = 8.7 Hz, 2H), 6.72 (s, 2H), 3.78 (s, 6H), 3.19 – 3.15 (m, 4H), 2.93 – 2.89 (m, 4H), 2.20 (s, 3H). HRMS (ESI) for $C_{25}H_{28}N_4O_3$ $[M + H]^+$: *m/z* = calcd, 433.2234; found, 433.2228.

5-(5-Chloro-4-methylpyridin-3-yl)-2-methoxybenzoic acid (11a)

The title compound was synthesized according to the procedure described for **6a** from 3-bromo-5-chloro-4-methylpyridine (**10**) (41 mg, 0.200 mmol) and 5-borono-2-methoxybenzoic acid (**9a**) (39 mg, 0.200 mmol). DMF (1.6 mL) and water (428 µL) were used as the solvents.

The crude material was used without purification in the subsequent cross-coupling reaction (56 mg, 87% yield). MS (ESI): *m/z* = 278.30 $[M + H]^+$, 280.30 $[M + H]^+ + 2$.

3-(5-Chloro-4-methylpyridin-3-yl)-5-methoxybenzoic acid (11b)

The title compound was synthesized according to the procedure described for **6a** from 3-bromo-5-chloro-4-methylpyridine (**10)** (41 mg, 0.200 mmol) and 3-carboxy-5-methoxyphenylboronic acid (**9b**) (39 mg, 0.200 mmol). DMF (1.6 mL) and water (428 µL) were used as the solvents. The crude material was used without purification in the subsequent cross-coupling reaction (56 mg, 90% yield). MS (ESI): *m/z* = 278.23 $[M + H]^+$, 280.30 $[M + H]^+ + 2$.

5-(5-(4-(4-(Tert-butoxycarbonyl)piperazin-1-yl)phenyl)-4-methylpyridin-3-yl)-2-methoxybenzoic acid (13a)

The title compound was synthesized according to the procedure described for **8a** from **11a** (56 mg, 0.200 mmol) and **1** (140 mg, 0.360 mmol). The crude product was purified by reverse-phase chromatography (2-95% ACN (0.1% formic acid) in water (0.1% formic acid)). The purified intermediate was used immediately in the subsequent reaction.

3-(5-(4-(4-(Tert-butoxycarbonyl)piperazin-1-yl)phenyl)-4-methylpyridin-3-yl)-5-methoxybenzoic acid (13b)

The title compound was synthesized according to the procedure described for **8a** from **11b** (56 mg, 0.200 mmol) and **1** (140 mg, 0.360 mmol). The crude product was purified by reverse-phase chromatography (2-95% ACN (0.1% formic acid) in water (0.1% formic acid)). The purified intermediate was used immediately in the subsequent reaction.

2-Methoxy-5-(4-methyl-5-(4-(piperazin-1-yl)phenyl)pyridin-3-yl)benzamide (14a)

The title compound was synthesized according to the procedure described for **5c** from **13a**. Deprotection with trifluoroacetic acid (459 µL, 6.00 mmol), purification by SPE and freeze drying

for 2 days afforded the final product as a yellow powder (5.96 mg, 7% yield over 4 steps). ^{1}H NMR (500 MHz, DMSO) δ 8.32 (s, 1H), 8.29 (s, 1H), 7.81 (d, *J* = 2.1 Hz, 1H), 7.71 (br s, 1H), 7.59 (br s, 1H), 7.56 (dd, *J* = 8.5, 2.2 Hz, 1H), 7.31 (d, *J* = 8.4 Hz, 2H), 7.26 (d, *J* = 8.6 Hz, 1H), 7.04 (d, *J* = 8.6 Hz, 2H), 3.95 (s, 3H), 3.21 – 3.18 (m, 4H), 2.97 – 2.93 (m, 4H), 2.14 (s, 3H). HRMS (ESI) for $C_{24}H_{26}N_4O_2$ $[M + H]^+$: *m/z* = calcd, 403.2129; found, 403.2126.

3-Methoxy-5-(4-methyl-5-(4-(piperazin-1-yl)phenyl)pyridin-3-yl)benzamide (14b)

The title compound was synthesized according to the procedure described for **5c** from **13b**. Deprotection with trifluoroacetic acid (0.459 ml, 6.00 mmol), purification by reverse-phase chromatography and SPE and freeze drying for 2 days afforded the final product as an off-white powder (4.52 mg, 6% yield over 4 steps). ^{1}H NMR (500 MHz, DMSO) δ 8.36 (s, 1H), 8.35 (s, 1H), 8.02 (br s, 1H), 7.52 – 7.49 (m, 1H), 7.49 – 7.47 (m, 1H), 7.44 (br s, 1H), 7.31 (d, *J* = 8.6 Hz, 2H), 7.17 – 7.15 (m, 1H), 7.05 (d, *J* = 8.7 Hz, 2H), 3.85 (s, 3H), 3.23 – 3.20 (m, 4H), 2.99 – 2.95 (m, 4H), 2.15 (s, 3H). HRMS (ESI) for $C_{24}H_{26}N_4O_2$ $[M + H]^+$: *m/z* = calcd, 403.2129; found, 403.2137.

Tert-butyl 4-(4-(5-chloro-4-methylpyridin-3-yl)phenyl)piperazine-1-carboxylate (15)

The title compound was synthesized according to the procedure described for **6a** from **10** (320 mg, 1.550 mmol) and **1** (722 mg, 1.860 mmol). The final product was an off-white crystalline solid (510 mg, 85% yield). ^{1}H NMR (500 MHz, $CDCl_3$) δ 8.48 (s, 1H), 8.30 (s, 1H), 7.21 (d, *J* = 8.7 Hz, 2H), 6.99 (d, *J* = 8.7 Hz, 2H), 3.63 – 3.59 (m, 4H), 3.24 – 3.19 (m, 4H), 2.33 (s, 3H), 1.49 (s, 9H). MS (ESI): *m/z* = 388.56 $[M + H]^+$, 390.57 $[M + H]^+ + 2$.

Tert-butyl 4-(4-(5-(3-methoxy-4-(methoxycarbonyl)phenyl)-4-methylpyridin-3-yl)phenyl)piperazine-1-carboxylate (17)

The title compound was synthesized according to the procedure described for **8a** from **15** (120 mg, 0.309 mmol) and 3-methoxy-4-methoxycarbonylphenylboronic acid, pinacol ester (**16**) (90 mg, 0.309 mmol). The solvents used were butan-1-ol (2 mL) and water (476 µL). The reaction mixture was diluted with water (20 mL) and extracted with EtOAc (3 x 20 mL). The combined organic fractions were dried over Na_2SO_4, filtered and concentrated under reduced pressure to afford a light beige solid (160 mg, 99% yield), which was used without further purification in the subsequent reaction. MS (ESI): *m/z* = 518.57 $[M + H]^+$.

Tert-butyl 4-(4-(5-(4-carbamoyl-3-methoxyphenyl)-4-methylpyridin-3-yl)phenyl)piperazine-1-carboxylate (M4K2149)

To a solution of **17** (0.160 g, 0.309 mmol) in MeOH (3.0 ml) at room temperature was added a solution of ammonia in MeOH (7N) (4.4 mL). The resulting mixture was heated to 75 °C for 3 days prior to cooling back down to room temperature, removing all solvents under reduced pressure, and triturating the residue from EtOAc with hexanes. The beige precipitate was collected by filtration and washed with hexanes. The product was subsequently dissolved in MeOH (5.0 mL) and treated with HCl (4.0 M in dioxane, 1.0 mL). The solution was stirred for 30 minutes prior to the removal of solvents under reduced pressure. The product was purified by SPE. The final compound was dried under vacuum overnight to give an off-white solid (75 mg, 60% yield). ^{1}H NMR (500 MHz, MeOD) δ 8.35 (s, 1H), 8.34 (s, 1H), 8.10 (d, *J* = 7.9 Hz, 1H), 7.33 (d, *J* = 8.6 Hz, 2H), 7.20 (s, 1H), 7.12 (d, *J* = 8.3 Hz, 3H), 4.04 (s, 3H), 3.32 – 3.26 (m, 4H), 3.13 – 3.07 (m, 4H), 2.24 (s, 3H). HRMS (ESI) for $C_{24}H_{26}N_4O_2$ $[M + H]^+$: *m/z* = calcd, 403.2129; found, 403.2128.

Tert-butyl 4-(4-(5-(3-methoxy-4-(methylcarbamoyl)phenyl)-4-methylpyridin-3-yl)phenyl)piperazine-1-carboxylate (18a)

To a solution of **17** (42 mg, 0.081 mmol) in MeOH (811 µL) was added methylamine, 33 wt. % in EtOH (1.0 mL). The solution was stirred at 85 °C for 5h. The solvents were removed under reduced pressure prior to the crude material being triturated from a minimum amount of EtOAc and hexanes. The product was filtered and dried under air, then dissolved in DCM (213 µL), treated with trifluoroacetic acid (100 µL, 1.310 mmol) and stirred for 1 hour. The solution was concentrated under reduced pressure prior to purification by reverse-phase (2-95% ACN (0.1% formic acid) in water (0.1% formic acid)). The product was purified by SPE. Freeze-drying for 2 days afforded a white powder (7.68 mg, 20% yield). ^{1}H NMR (500 MHz, MeOD) δ 8.32 (s, 1H), 8.30 (s, 1H), 8.01 (d, *J* = 7.9 Hz, 1H), 7.30 (d, *J* = 8.6 Hz, 2H), 7.15 (s, 1H), 7.12 – 7.06 (m, 3H), 4.00 (s, 3H), 3.30 – 3.27 (m, 4H), 3.12 – 3.08 (m, 4H), 2.98 (s, 3H), 2.21 (s, 3H). HRMS (ESI$^+$) for $C_{25}H_{28}N_4O_2$ $[M + H]^+$: *m/z* = calcd, 417.2285; found, 417.2288.

4-(5-(4-(4-(Tert-butoxycarbonyl)piperazin-1-yl)phenyl)-4-methylpyridin-3-yl)-2-methoxybenzoic acid

To a suspension of **17** (54 mg, 0.104 mmol) in THF (695 µL) and water (695 µL) was added potassium hydroxide pellets (12 mg, 0.209 mmol). The suspension was stirred at room temperature for 2 h. The reaction mixture was diluted with water (35 mL) and extracted with Et_2O (1 x 20 mL). The aqueous layer was carefully acidified to a pH of 5 and extracted with DCM (3 x 20 mL). The Et_2O and DCM layers were combined, dried over $MgSO_4$, filtered and concentrated under reduced pressure to afford an off-white solid (50 mg, 93% yield). MS (ESI): *m/z* = 504.60 $[M + H]^+$.

2-Methoxy-N,N-dimethyl-4-(4-methyl-5-(4-(piperazin-1-yl)phenyl)pyridin-3-yl)benzamide (18b)

To a solution of 4-(5-(4-(4-(Tert-butoxycarbonyl)piperazin-1-yl)phenyl)-4-methylpyridin-3-yl)-2-methoxybenzoic acid (50 mg, 0.099 mmol), HOBt (16 mg, 0.119 mmol) and EDC (18 mg, 0.119 mmol) in DCM (894 µL) and DMF (99 µL) was added DIPEA (43 µL, 0.248 mmol) and dimethylamine, 2.0 M in THF (50 µL, 0.099 mmol). The solution was stirred at 50 ºC overnight. The reaction mixture was diluted with water (5 mL) and DCM (5 mL). The organic layer was separated, dried over $MgSO_4$, filtered and concentrated under reduced pressure to afford a sticky yellow solid. The solid was dissolved in DCM (886 µL) and treated with trifluoroacetic acid (339 µL, 4.430 mmol). The solution was stirred for 45 minutes prior to purification by reverse-phase (2-95% ACN (0.1% formic acid) in water (0.1% formic acid)). The product was purified by SPE. Freeze-drying for 2 days afforded a white powder (13 mg, 23% yield). ^{1}H NMR (500 MHz, MeOD) δ 8.33 – 8.30 (m, 2H), 7.35 – 7.28 (m, 3H), 7.12 – 7.04 (m, 4H), 3.90 (s, 3H), 3.28 – 3.24 (m, 4H), 3.12 (s, 3H), 3.08 – 3.04 (m, 4H), 2.94 (s, 3H), 2.22 (s, 3H). HRMS (ESI) for $C_{25}H_{28}N_4O_2$ $[M + H]^+$: *m/z* = calcd, 431.2442; found, 431.2439.

4-Bromo-2-(hydroxymethyl)benzonitrile

To a solution of 4-bromo-2-formylbenzonitrile (630 mg, 3.00 mmol) in MeOH (7.5 mL) cooled in an ice bath was added sodium borohydride (125 mg, 3.30 mmol). The reaction mixture was stirred for an hour at 0 °C prior to quenching with water (20 mL). Volatiles were removed under reduced pressure and the aqueous layer was extracted with EtOAc (3 x 50 mL). The combined organic fractions were washed with brine, dried over $NaSO_4$, filtered and concentrated under reduced pressure to afford a yellow-brown solid, which was used without further purification in the subsequent reaction (637 mg, 85% yield). MS (ESI): *m/z* = 212.28 $[M + H]^+$, 214.22 $[M + H]^+$ + 2.

4-bromo-2-(methoxymethyl)benzonitrile

To a solution of 4-bromo-2-(hydroxymethyl)benzonitrile (400 mg, 1.89 mmol) in THF (6.3 mL) cooled in an ice bath was added sodium hydride, 60% in mineral oil (181 mg, 7.54 mmol). The solution was stirred for 30 min prior to the addition of iodomethane (1.4 mL, 22.63 mmol). The reaction mixture was stirred for an additional 2 h, then quenched with water (50 mL) and extracted with EtOAc (3 x 50 mL). The combined organic fractions were dried over Na_2SO_4, filtered and concentrated under reduced pressure prior to purification by silica gel chromatography (0-80% EtOAc in hexanes) to afford the final product (89 mg, 20% yield).

4-bromo-2-(methoxymethyl)benzamide

The title compound was synthesized according to the procedure described for **5d** from 4-bromo-2-(methoxymethyl)benzonitrile (80 mg, 0.354 mmol). The reaction mixture was stirred at 90 ^oC for 2 h then at room temperature overnight. The crude mixture was diluted with water (10 mL) and extracted with EtOAc (3 x 10 mL). The organic layers were combined and dried over Mg_2SO_4 to afford an off-white solid (71 mg, 81% yield). ^1H NMR (500 MHz, DMSO) δ 7.84 (br s, 1H), 7.64 (d, *J* = 1.9 Hz, 1H), 7.55 (dd, *J* = 8.2, 2.0 Hz, 1H), 7.46 (br s, 1H), 7.42 (d, *J* = 8.2 Hz, 1H), 4.58 (s, 2H).

2-(Methoxymethyl)-4-(4,4,5,5-tetramethyl-1,3,2-dioxaborolan-2-yl)benzamide (19c)

The title compound was synthesized according to the procedure described for **4a** from 4-bromo-2-(methoxymethyl)benzamide (50 mg, 0.205 mmol). The dark brown supernatant was used without purification in the subsequent reaction (60 mg, 78% yield). MS (ESI): *m/z* = 292.53 $[M + H]^+$.

4-bromo-2-chloro-6-fluorobenzonitrile

The title compound was prepared using a modified literature procedure.[36] To a solution of 4-bromo-2-chloro-6-fluoroaniline (2.00 g, 8.91 mmol) in DCM (17.8 mL) was added nitrosonium

tetrafluoroborate (1.14 g, 9.80 mmol). The solution was stirred for 1 h at room temperature, then cooled in an ice bath. Potassium cyanide (1.16 g, 17.82 mmol) was added. A solution of copper (II) sulfate pentahydrate (4.45 g, 17.82 mmol) in water (35.0 mL) was then added gradually. The suspension was stirred for 1 hour on ice, then at room temperature for an additional hour. The reaction mixture was diluted with DCM and saturated sodium bicarbonate solution, then filtered through celite. The organic layer was washed with brine, separated, dried over Na_2SO_4, filtered and concentrated under reduced pressure prior to purification by silica gel chromatography (0-50% EtOAc in hexanes) to give the final product (0.398 g, 10% yield).

4-bromo-2-chloro-6-methoxybenzonitrile

The title compound was prepared using a modified literature procedure.[37] To a solution of 4-bromo-2-chloro-6-fluorobenzonitrile (0.398 g, 1.697 mmol) in 1,4-dioxane (4.6 mL) was added MeOH (178 µL, 4.412 mmol). Sodium hydride, 60% in mineral oil (106 mg, 4.412 mmol) was added gradually over 1 h. The reaction mixture was stirred for 1 hour at room temperature. The solvents were removed under reduced pressure and the crude material was suspended in water and filtered. The filter cake was dissolved in DCM, concentrated and purified by silica gel chromatography (0-100% DCM in hexanes) to give the final product (223 mg, 49% yield). MS (ESI): *m/z* = 246.26 $[M + H]^+$, 248.26 $[M + H]^+ + 2$, 250.21 $[M + H]^+ + 4$. ^{1}H NMR (500 MHz, $CDCl_3$) δ 7.27 (d, *J* = 1.5 Hz, 1H), 7.04 (d, *J* = 1.4 Hz, 1H), 3.95 (s, 3H).

4-bromo-2-chloro-6-methoxybenzamide

4-bromo-2-chloro-6-methoxybenzamide was synthesized according to the procedure described for **5d** from 4-bromo-2-chloro-6-methoxybenzonitrile (219 mg, 0.889 mmol). The solution was stirred at 90 ^{o}C for 6 h. The crude was diluted with water (50 mL) and extracted with EtOAc (3 x 50 mL). The organic layers were combined, dried over Na_2SO_4, filtered and concentrated under

reduced pressure to give the final product (219 mg, 77% yield). MS (ESI): *m/z* = 264.25 [M + H]$^+$, 266.26 [M + H]$^+$ + 2, 268.20 [M + H]$^+$ + 4. ^{1}H NMR (500 MHz, $CDCl_3$) δ 7.20 (d, *J* = 1.4 Hz, 1H), 6.99 (d, *J* = 1.3 Hz, 1H), 5.93 (br s, 1H), 5.72 (br s, 1H), 3.85 (s, 3H).

2-Chloro-6-methoxy-4-(4,4,5,5-tetramethyl-1,3,2-dioxaborolan-2-yl)benzamide (19e)

The title compound was synthesized according to the procedure described for **4a** from 4-bromo-2-chloro-6-methoxybenzamide (100 mg, 0.378 mmol). The dark supernatant was used without purification in the subsequent reaction (113 mg, 36% yield). MS (ESI): *m/z* = 312.46 [M + H]$^+$, 314.41 [M + H]$^+$ + 2.

5-(4-Methyl-5-(4-(piperazin-1-yl)phenyl)pyridin-3-yl)isoindolin-1-one (20a)

The title compound was synthesized according to the procedure described for **8a** from **15** (75 mg, 0.193 mmol) and 5-(4,4,5,5-Tetramethyl-1,3,2-dioxaborolan-2-yl)isoindolin-1-one (**19a**) (50 mg, 0.193 mmol). The final product was a white powder (33 mg, 44% yield). ^{1}H NMR (500 MHz, DMSO) δ 8.62 (br s, 1H), 8.37 (s, 1H), 8.34 (s, 1H), 7.77 (d, *J* = 7.8 Hz, 1H), 7.65 (s, 1H), 7.54 (d, *J* = 7.7 Hz, 1H), 7.31 (d, *J* = 8.7 Hz, 2H), 7.04 (d, *J* = 8.8 Hz, 2H), 4.44 (s, 2H), 3.19 – 3.16 (m, 4H), 2.94 – 2.90 (m, 4H), 2.15 (s, 3H). HRMS (ESI) for $C_{24}H_{24}N_4O$ [M + H]$^+$: *m/z* = calcd, 385.2023; found, 385.2018.

4-(4-Methyl-5-(4-(piperazin-1-yl)phenyl)pyridin-3-yl)benzamide (20b)

The title compound was synthesized according to the procedure described for **8a** from **15** (19 mg, 0.048 mmol) and 4-aminocarbonylphenylboronic acid (**19b**) (8 mg, 0.048 mmol). The final product was a light pink-orange powder (8 mg, 45% yield). ^{1}H NMR (500 MHz, DMSO) δ 8.36 (s, 1H), 8.33 (s, 1H), 8.06 (br s, 1H), 7.98 (d, *J* = 8.3 Hz, 2H), 7.53 (d, *J* = 8.2 Hz, 2H), 7.42 (br s,

1H), 7.31 (d, *J* = 8.5 Hz, 2H), 7.05 (d, *J* = 8.7 Hz, 2H), 3.23 – 3.19 (m, 4H), 3.02 – 2.92 (m, 4H), 2.15 (s, 3H). HRMS (ESI) for $C_{23}H_{24}N_4O$ $[M + H]^+$: *m/z* = calcd, 373.2023; found, 373.2014.

2-(Methoxymethyl)-4-(4-methyl-5-(4-(piperazin-1-yl)phenyl)pyridin-3-yl)benzamide (20c)

The title compound was synthesized according to the procedure described for **8a** from **15** (73 mg, 0.188 mmol) and **19c** (60 mg, 0.205 mmol). The final compound was an off-white powder (23 mg, 29% yield). ^{1}H NMR (500 MHz, $CDCl_3$) δ 8.45 (s, 1H), 8.37 (s, 1H), 7.93 (d, *J* = 7.9 Hz, 1H), 7.44 (dd, *J* = 7.9, 1.7 Hz, 1H), 7.40 (d, *J* = 1.4 Hz, 1H), 7.28 – 7.26 (m, 2H), 7.01 (d, *J* = 8.7 Hz, 2H), 5.74 (br s, 1H), 4.65 (s, 2H), 3.46 (s, 3H), 3.26 – 3.22 (m, 4H), 3.10 – 3.06 (m, 4H), 2.17 (s, 3H). HRMS (ESI) for $C_{25}H_{28}N_4O_2$ $[M + H]^+$: *m/z* = calcd, 417.2285; found, 417.2283.

2-Fluoro-4-(4-methyl-5-(4-(piperazin-1-yl)phenyl)pyridin-3-yl)benzamide (20d)

The title compound was synthesized according to the procedure described for **8a** from **15** (100 mg, 0.258 mmol) and 4-carbamoyl-3-fluorophenylboronic acid (**19d**) (47 mg, 0.258 mmol). The final compound was a white powder (50 mg, 50% yield). ^{1}H NMR (500 MHz, MeOD) δ 8.37 (s, 1H), 8.32 (s, 1H), 7.96 (t, *J* = 8.0 Hz, 1H), 7.38 – 7.30 (m, 4H), 7.11 (d, *J* = 8.7 Hz, 2H), 3.29 – 3.23 (m, 4H), 3.08 – 3.02 (m, 4H), 2.24 (s, 3H). ^{19}F NMR (471 MHz, MeOD) δ -114.60. HRMS (ESI) for $C_{23}H_{23}FN_4O$ $[M + H]^+$: *m/z* = calcd, 391.1929; found, 391.1926.

2-Chloro-6-methoxy-4-(4-methyl-5-(4-(piperazin-1-yl)phenyl)pyridin-3-yl)benzamide (20e)

The title compound was synthesized according to the procedure described for **6a** from **3** (66 mg, 0.153 mmol) and **19e** (59 mg, 0.189 mmol). The material was deprotected with trifluoroacetic acid (350 µL, 4.579 mmol) and purified by SPE. Freeze-drying for a day and a half afforded an off-white powder (24 mg, 36% yield). ^{1}H NMR (500 MHz, $CDCl_3$) δ 8.45 (s, 1H), 8.31 (s, 1H), 7.26 – 7.24 (m, 2H), 7.03 (d, *J* = 1.1 Hz, 1H), 7.01 (d, *J* = 8.7 Hz, 2H), 6.81 (d, *J* = 1.0 Hz, 1H),

5.94 – 5.87 (br m, 2H), 3.89 (s, 3H), 3.26 – 3.22 (m, 4H), 3.10 – 3.06 (m, 4H), 2.18 (s, 3H). HRMS (ESI) for $C_{24}H_{25}ClN_4O_2$ $[M + H]^+$: *m/z* = calcd, 437.1739; found, 437.1740.

4-Bromo-2-fluoro-6-methoxybenzonitrile (22a) and 4-bromo-2,6-dimethoxybenzonitrile (22b)

The title compounds were prepared according to the procedure described for 4-bromo-2-chloro-6-methoxybenzonitrile from 4-bromo-2,6-difluorobenzonitrile (**21**) (2.00 g, 9.17 mmol), MeOH (744 µL, 18.34 mmol) and sodium hydride, 60% in mineral oil (0.733 g, 18.34 mmol). 4-bromo-2-fluoro-6-methoxybenzonitrile was a white crystalline solid (965 mg, 46% yield). 4-bromo-2,6-dimethoxybenzonitrile was also a white crystalline solid (754 mg, 34% yield). 4-bromo-2-fluoro-6-methoxybenzonitrile : ^{1}H NMR (500 MHz, $CDCl_3$) δ 7.00 (d, *J* = 8.0 Hz, 1H), 6.94 (s, 1H), 3.95 (s, 3H). ^{19}F NMR (471 MHz, $CDCl_3$) δ -103.78 (s). MS (ESI): *m/z* = 230.21 $[M + H]^+$, 232.21 $[M + H]^+ + 2$. 4-bromo-2,6-dimethoxybenzonitrile: ^{1}H NMR (500 MHz, $CDCl_3$) δ 6.73 (s, 2H), 3.91 (s, 6H). MS (ESI): *m/z* = 242.25 $[M + H]^+$, 244.19 $[M + H]^+ + 2$.

(4-Carbamoyl-3-fluoro-5-methoxyphenyl)boronic acid (23a)

The title compound was synthesized according to the procedure described for **4a** from **5d** (2.48 g, 10.0 mmol). The dark brown supernatant was used without further purification in subsequent reactions (2.46 g, 84% yield). MS (ESI): *m/z* = 214.34 $[M + H]^+$.

2,6-Dimethoxy-4-(4,4,5,5-tetramethyl-1,3,2-dioxaborolan-2-yl)benzamide (23b)

The title compound was synthesized according to the procedure described for **4a** from **5e** (800 mg, 3.08 mmol). The dark brown supernatant was used without further purification in subsequent reactions (945 mg, 70% yield). MS (ESI): *m/z* = 308.26 $[M + H]^+$.

4-(5-Chloro-4-methylpyridin-3-yl)-2-fluoro-6-methoxybenzamide (24a)

The title compound was synthesized according to the procedure described for **6a** from **10** (2.06 g, 10.0 mmol) and **23a** (2.95g, 10.0 mmol). The final compound was an off-white crystalline solid (1.67 g, 56% yield). ^{1}H NMR (500 MHz, DMSO) δ 8.63 (s, 1H), 8.38 (s, 1H), 7.90 (br s, 1H), 7.60 (br s, 1H), 6.97 – 6.94 (m, 2H), 3.83 (s, 3H), 2.33 (s, 3H). ^{19}F NMR (471 MHz, DMSO) δ -116.46. MS (ESI): *m/z* = 294.97 $[M + H]^+$, 297.10 $[M + H]^+ + 2$.

4-(5-Chloro-4-methylpyridin-3-yl)-2,6-dimethoxybenzamide (24b)

The title compound was synthesized according to the procedure described for **6a** from **10** (954 mg, 4.62 mmol) and **23b** (946 mg, 3.08 mmol). The final compound was an off-white crystalline solid (747 mg, 79% yield). ^{1}H NMR (500 MHz, DMSO) δ 8.61 (s, 1H), 8.38 (s, 1H), 7.58 (br s, 1H), 7.26 (br s, 1H), 6.70 (s, 2H), 3.77 (s, 6H), 2.34 (s, 3H). MS (ESI): *m/z* = 307.26 $[M + H]^+$.

(2R,6S)-4-(4-bromophenyl)-1,2,6-trimethylpiperazine

The title compound was prepared using modified literature procedures.[38-39] A solution of (2*R*,6*S*)-1,2,6-trimethylpiperazine (100 mg, 0.780 mmol), 1-bromo-4-iodobenzene (221 mg, 0.780 mmol), bis(dibenzylideneacetone)palladium(0) (22 mg, 0.039 mmol), Xantphos (68 mg, 0.117 mmol) and lithium tert-butoxide 1.0 M in THF (2.34 mL, 2.340 mmol) in 1,4-Dioxane (3.12 mL) was heated to 110 ^{o}C and stirred overnight. Volatiles were removed under reduced pressure and the crude material was purified by silica gel chromatography (0-10% MeOH in EtOAc). ^{1}H NMR (500 MHz, MeOD) δ 7.32 (d, *J* = 9.0 Hz, 2H), 6.87 (d, *J* = 9.0 Hz, 2H), 3.55 – 3.49 (m, *J* = 11.5 Hz, 2H), 2.52 – 2.46 (m, *J* = 11.4 Hz, 2H), 2.44 – 2.38 (m, 2H), 2.33 (s, 3H), 1.19 (d, *J* = 6.1 Hz, 6H). MS (ESI): *m/z* = 283.37 $[M + H]^+$, 285.32 $[M + H]^+ + 2$.

(2R,6S)-1,2,6-trimethyl-4-(4-(4,4,5,5-tetramethyl-1,3,2-dioxaborolan-2-yl)phenyl)piperazine (25c)

The title compound was prepared according to the procedure described for **6a** from (2*R*,6*S*)-4-(4-bromophenyl)-1,2,6-trimethylpiperazine (100 mg, 0.353 mmol). The dark brown reaction mixture was used without purification in subsequent reactions (117 mg, 91% yield). MS (ESI): *m/z* = 331.46 $[M + H]^+$.

2-Fluoro-6-methoxy-4-(4-methyl-5-(4-(4-methylpiperazin-1-yl)phenyl)pyridin-3-yl)benzamide (26a)

The title compound was synthesized according to the procedure described for **6a** from **24a** (150 mg, 0.509 mmol) and 4-(4-Methylpiperazin-1-yl)phenylboronic acid (**25a**) (134 mg, 0.611 mmol). XPhos Pd G3 (21.54 mg, 0.025 mmol) was used as the catalyst. The reaction mixture was adsorbed onto celite and the solvents were removed under reduced pressure. The crude material was purified by silica gel chromatography (0-15% MeOH in EtOAc). Freeze drying for 1 day afforded a white powder (183 mg, 83% yield). ^{1}H NMR (500 MHz, DMSO) δ 8.37 (s, 1H), 8.34 (s, 1H), 7.89 (br s, 1H), 7.58 (br s, 1H), 7.30 (d, *J* = 8.7 Hz, 2H), 7.05 (d, *J* = 8.8 Hz, 2H), 6.98 – 6.94 (m, 2H), 3.85 (s, 3H), 3.23 – 3.19 (m, 4H), 2.48 – 2.45 (m, 4H), 2.23 (s, 3H), 2.19 (s, 3H). ^{19}F NMR (471 MHz, DMSO) δ -116.74. HRMS (ESI) for $C_{25}H_{27}FN_4O_2$ $[M + H]^+$: *m/z* = calcd, 435.2191; found, 435.2191.

2-Fluoro-4-(5-(4-(4-isopropylpiperazin-1-yl)phenyl)-4-methylpyridin-3-yl)-6-methoxybenzamide (26b)

The title compound was synthesized according to the procedure described for **26a** from **24a** (150 mg, 0.509 mmol) and 4-(4-Isopropylpiperazinyl)phenylboronic acid, pinacol ester (**25b**) (202 mg, 0.611 mmol). The final compound was a white powder (142 mg, 60% yield). ^{1}H NMR (500 MHz, DMSO) δ 8.38 (s, 1H), 8.34 (s, 1H), 7.89 (br s, 1H), 7.58 (br s, 1H), 7.30 (d, *J* = 8.7 Hz, 2H), 7.04 (d, *J* = 8.8 Hz, 2H), 6.98 – 6.95 (m, 2H), 3.85 (s, 3H), 3.23 – 3.17 (m, 4H), 2.72 – 2.66 (m, 1H), 2.63 – 2.57 (m, 4H), 2.19 (s, 3H), 1.02 (d, *J* = 6.5 Hz, 6H). ^{19}F NMR (471 MHz, DMSO) δ -116.74. HRMS (ESI) for $C_{27}H_{31}FN_4O_2$ $[M + H]^+$: *m/z* = calcd, 463.2504; found, 463.2506.

2-Fluoro-6-methoxy-4-(4-methyl-5-(4-((3R,5S)-3,4,5-trimethylpiperazin-1-yl)phenyl)pyridin-3-yl)benzamide (26c)

The title compound was synthesized according to the procedure described for **26a** from **24a** (156 mg, 0.531 mmol) and (2*R*,6*S*)-1,2,6-trimethyl-4-(4-(4,4,5,5-tetramethyl-1,3,2-dioxaborolan-2-yl)phenyl)piperazine (**25c**) (58.5 mg, 0.177 mmol). The final compound was a light yellow powder (36 mg, 43% yield). ^{1}H NMR (500 MHz, $CDCl_3$) δ 8.43 (s, 1H), 8.30 (s, 1H), 7.24 (d, *J* = 8.6 Hz, 2H), 6.99 (d, *J* = 8.6 Hz, 2H), 6.77 (dd, *J* = 9.7, 0.5 Hz, 1H), 6.71 (s, 1H), 6.32 (br s, 1H), 6.09 (br s, 1H), 3.91 (s, 3H), 3.57 (d, *J* = 11.5 Hz, 2H), 2.86 – 2.67 (m, 2H), 2.60 – 2.45 (m, 2H), 2.40 (s, 3H), 2.16 (s, 3H), 1.26 (d, *J* = 5.8 Hz, 6H). ^{19}F NMR (471 MHz, MeOD) δ -117.13. HRMS (ESI) for $C_{27}H_{31}FN_4O_2$ $[M + H]^+$: *m/z* = calcd, 463.2504; found, 463.2510.

2,6-Dimethoxy-4-(4-methyl-5-(4-(4-methylpiperazin-1-yl)phenyl)pyridin-3-yl)benzamide (26d)

The title compound was synthesized according to the procedure described for **26a** from **24b** (150 mg, 0.489 mmol) and **25a** (129 mg, 0.587 mmol). The final compound was a white powder (189 mg, 87% yield). ^{1}H NMR (500 MHz, DMSO) δ 8.35 (s, 1H), 8.35 (s, 1H), 7.57 (br s, 1H), 7.30

(d, *J* = 8.6 Hz, 2H), 7.23 (br s, 1H), 7.05 (d, *J* = 8.7 Hz, 2H), 6.72 (s, 2H), 3.78 (s, 6H), 3.23 – 3.19 (m, 4H), 2.48 – 2.46 (m, 4H), 2.24 (s, 3H), 2.20 (s, 3H). HRMS (ESI) for $C_{26}H_{30}N_4O_3$ $[M + H]^+$: *m/z* = calcd, 477.2391; found, 447.2394.

4-(5-(4-(4-Isopropylpiperazin-1-yl)phenyl)-4-methylpyridin-3-yl)-2,6-dimethoxybenzamide (26e)

The title compound was synthesized according to the procedure described for **26a** from **24b** (150 mg, 0.489 mmol) and **25b** (194 mg, 0.587 mmol). The final compound was an off-white powder (179 mg, 75% yield). ^{1}H NMR (500 MHz, MeOD) δ 8.31 (s, 1H), 8.30 (s, 1H), 7.33 (d, *J* = 8.6 Hz, 2H), 7.13 (d, *J* = 8.7 Hz, 2H), 6.69 (s, 2H), 3.86 (s, 6H), 3.47 – 3.36 (m, 4H), 3.15 – 3.01 (m, 5H), 2.22 (s, 3H), 1.27 (d, *J* = 6.6 Hz, 6H). HRMS (ESI) for $C_{28}H_{34}N_4O_3$ $[M + H]^+$: *m/z* = calcd, 475.2704; found, 475.2705.

2,6-Dimethoxy-4-(4-methyl-5-(4-((3R,5S)-3,4,5-trimethylpiperazin-1-yl)phenyl)pyridin-3-yl)benzamide (26f)

The title compound was synthesized according to the procedure described for **26a** from **24b** (109 mg, 0.354 mmol) and **25c** (58 mg, 0.177 mmol). The final compound was a white powder (22 mg, 26% yield). ^{1}H NMR (500 MHz, MeOD) δ 8.31 (s, 1H), 8.29 (s, 1H), 7.30 (d, *J* = 8.4 Hz, 2H), 7.09 (d, *J* = 8.5 Hz, 2H), 6.69 (s, 2H), 3.86 (s, 6H), 3.65 (d, *J* = 11.8 Hz, 2H), 2.62 – 2.55 (m, 2H), 2.51 – 2.44 (m, 2H), 2.37 (s, 3H), 2.23 (s, 3H), 2.16 (s, 2H), 1.23 (d, *J* = 6.2 Hz, 6H). HRMS (ESI) for $C_{28}H_{34}N_4O_3$ $[M + H]^+$: *m/z* = calcd, 475.2704; found, 475.2699.

Kinase Assay

The biochemical potencies of all compounds were measured by Reaction Biology Corporation (RBC) (Malvern, Pennsylvania, United States). Compounds were tested against ALK2/ACVR1 and ALK5/TGFβ-R1 in a 10-dose IC_{50} mode with a 2-fold serial dilution starting at 1, 2 or 5 µM. Reactions were conducted at an ATP concentration of 10 µM and Casein concentration of 1 mg/mL. LDN-193189 was tested as a control in a 10-dose IC_{50} mode with a 3-fold serial dilution starting at 10 µM. Reductions in enzymatic activity were determined relative to DMSO controls.

Cell Culture and Transfection

HEK-293 cells were maintained in DMEM medium (Gibco) supplemented with 10% fetal bovine serum (FBS) (Thermo Fisher), and penicillin/ streptomycin (Thermo Fisher). HEK-293 cells were transfected with protein expression or reporter constructs using FuGENE HD (Promega) according to the manufacturer's instructions. Briefly, DNA was diluted into phenol red-free Opti-MEM (Gibco) at a concentration of 10 µg/mL. Without coming in contact with the sides of the container, 3µL FuGENE HD was added for each µg of DNA used. After thorough mixing by inversion, FuGENE HD/DNA complexes were allowed to form by incubation at room temperature for 20 min. 1 part of transfection mixture was added to 20 parts of HEK-293 cell suspension with a density of 200,000 cells per mL (volume/volume). HEK-293 cells were incubated in a humidified, 37°C incubator with 5% carbon dioxide for 24 h before they are used in the NanoBRET target engagement assay or dual luciferase reporter assay.

NanoBRET Target Engagement Assay

ALK2-C-terminal nanoluciferase fusion with GSSG linker was encoded by pFC32K vector (Promega). 1 part of ALK2-nanoluciferase fusion construct was mixed with 9 parts of Transfection Carrier DNA (mass/mass) (Promega). Transfected cells were trypsinised and resuspended in Opti-

MEM at a density of 200,000 cells per mL. 17 µL of cells were dispensed into each well of 384-well flat bottom polypropylene plate (Greiner). 20X working solution of target engagement tracer PBI-6908 (Promega) was prepared by diluting DMSO stock in tracer dilution buffer (12.5mM HEPES pH7.5, 31.25% PEG-400). 1000X stocks of test compounds in DMSO (Cell Signalling Technology) were diluted further in Opti-MEM for 10X working solutions. After the addition of 1 µL of 20X target engagement tracer and 2 µL of 10X working solutions, contents of the wells were thoroughly mixed by agitating the plate at 500 rpm for 1 minute. Cells were incubated in a humidified, 37°C incubator with 5% carbon dioxide for 2 h prior to BRET measurement. For bioluminiscence resonance energy transfer (BRET) measurement, NanoBRET NanoGlo Substrate and Extracellular NanoLuc Inhibitor (Promega) was diluted 166X and 500X, respectively, in Opti-MEM to produce 3X working stock. A PHERAstar FSX microplate reader (BMG Labtech) with LUM 610-LP 460-80 optical module was used to measure the intensity of the dual emission. A measurement interval of 1 sec and gain settings of 3600 and 1879 for 610 nm and 460 nm respectively were used. Milli-BRET units (mBU) were calculated by dividing the signal measured at 610 nm with the signal measured at 460 nm and multiplying by 1000. The apparent EC_{50} values of test compounds were estimated using the [Inhibitor] vs. response (three parameters) non-linear regression curve fitting function of GraphPad Prism 7.

Dual Luciferase Reporter Assay

CAGA-Luc and Renilla-luciferase constructs (a gift of Dr Petra Knaus, Free University of Berlin) were used as the reporter for ALK5 signalling and loading control respectively. 4 parts of CAGA-Luc construct was mixed with 1 part of Renilla-luciferase construct (mass/mass). 10,000 transfected cells were seeded into each well of 96-well plate (Corning). 24 h after transfection, the cells were incubated with 10 ng/mL TGF-β1 (Peprotech, 100-21-10) and test compounds

simultaneously at the concentrations indicated in a humidified, 37°C incubator with 5% carbon dioxide. 24 h later, cells were harvested, lysed and processed for measurement of luciferase activity using the Dual-Luciferase Reporter Assay System (Promega) according to the manufacturer's instructions. Briefly, culture medium was aspirated completely and cells were lysed in 50 µl of 1X PLB with 300 rpm agitation for 30 min. 10 µL of cell lysate was dispensed into each well of a 384-well flat bottom polypropylene plate (Greiner). Luminescent signal of firefly and Renilla luciferase activity were measured sequentially using a PHERAstar FS microplate reader (BMG Labtech) after the addition of 25 µL of LARII and Stop & Glo respectively. A measurement interval of 2 sec and gain setting of 3600 were used. Firefly luciferase signal was normalised to cell number by division with Renilla luciferase signal. Relative luciferase unit (RLU) was obtained by further division with signal from cells without TGF-β stimulation. The apparent EC50 values of test compounds were estimated using the [Inhibitor] vs. response (three parameters) non-linear regression curve fitting function of GraphPad Prism 7.

Caco-2 Permeability Assay

Caco-2 cells (C2BBe1) were purchased from American Type Culture Collection, ATCC. Caco-2 cell cultures were routinely maintained in T-75 tissue culture flasks in Dulbecco's Modified Eagle Medium (DMEM) containing 20% FBS, 0.1mg/mL normocin and 0.05mg/mL gentamicin. These cells were seeded at a density of 40,000 cells/well on 24 well polyethylene terephthalate (PET) membrane (1.0 µm pore size, 0.31 cm^2 surface area) insert plates. Cell monolayers were grown for 21 or 22 days at 37°C with 5% CO_2 in a humidified incubator. The cell culture medium was replaced twice weekly during the cell growth period. Prior to beginning the permeability assay, cell monolayers were rinsed with Hank's Balanced Salt Solution (HBSS) twice to remove residual cell culture medium.

The assay buffer was comprised of HBSS containing 10 mM HEPES and 15 mM glucose at a pH of 7.4. The dosing buffer contained 5 µM metoprolol (positive control), 5 µM atenolol (negative control) and 100 µM Lucifer yellow in the assay buffer. The receiving buffer contained 1% bovine serum albumin (BSA) in the assay buffer. The concentration of test compound was 5 µM in the dosing buffer (final DMSO concentration was 0.1%). Digoxin at 10 µM was utilized as a Pgp substrate control.

For apical to basolateral (A to B) permeability experiment, 0.25 mL of the dosing buffer was added to the apical chambers and 1.0 mL of receiving buffer was added to the basolateral chambers of the assay plate. For basolateral to apical (B to A) permeability experiment, 0.25 mL of the receiving buffer was added to the apical chambers and 1.0 mL of dosing buffer was added to the basolateral chambers of the assay plates. The assay plates were then incubated at 37°C for 120 minutes on an orbital shaker at 65 rpm. Sample solutions were taken from the donor chambers (10 µL) and receiver chambers (100 µL) after the incubation period. For each sample there were two technical replicates. The sample solutions from donor chambers were diluted ten-times with receiving buffer. In order to extract test compounds and precipitate BSA from sample solutions, three volumes of acetonitrile (containing 0.5% formic acid and an internal standard) were added and the plate was vigorously mixed. Sample solutions were then centrifuged at 4,000 rpm for 10 minutes to remove debris and precipitated BSA. Approximately 150 µL of supernatant was subsequently transferred to a new 96 well microplate for LC/MS analysis. Narrow-window mass extraction LC/MS analysis was performed for all samples from this study using a Waters Xevo quadrupole time-of-flight (QTof) mass spectrometer to determine relative peak areas of parent compounds. The co-dosed positive and negative controls were also measured for each well to

monitor integrity of cell monolayers and well-to-well variability. The apparent permeability coefficient (P_{app}) and post assay recovery are calculated using the following equations:

$P_{app} = V_r \times (dC/dt) \times 1/(A \times C_0)$

Percent Recovery = $100 \times ((V_r \times C_r^{final}) + (V_d \times C_d^{final}))/(V_d \times C_0)$

Where,

dC/dt is the slope of the cumulative concentration in the receiver compartment versus time

V_r is the volume of the receiver compartment

V_d is the volume of the donor compartment

A is the membrane surface area

C_0 is the compound initial concentration in the donor chamber

C_r^{final} is the cumulative receiver concentration at the end of the incubation period

C_d^{final} is the concentration of the donor at the end of the incubation period

Efflux ratio (ER) is defined as P_{app} (B-to-A) / P_{app} (A-to-B).

Liver Microsomal Metabolic Stability Assay

For this assay, stock solutions of test compounds in DMSO (1 mM) were initially diluted to a concentration of 40.0 µM using 0.1 M potassium phosphate buffer (pH 7.4). Test compounds were then added to reaction wells at a final concentration of 1 µM which was assumed to be well below Km values to ensure linear reaction conditions (i.e. avoid saturation). The final DMSO concentration was kept constant at 0.1%. Each compound was tested in duplicate for both time points (0 and 60 minutes). CD-1 mouse (male) or pooled human liver microsomes (Corning Gentest) were added to the reaction wells at a final concentration of 0.5 mg/mL (protein). The final volume for each reaction was 100 µL, which included the NADPH-Regeneration Solution

(NRS) mix (Corning Gentest). This NRS mix was comprised of glucose 6-phosphate dehydrogenase, $NADP^+$, $MgCl_2$, and glucose 6-phosphate. Reactions were carried out at 37°C in an orbital shaker at 175 rpm. Upon completion of the 60-minute time point, reactions were terminated by the addition of 2-volumes (200 µL) of ice-cold acetonitrile containing 0.5% formic acid and an internal standard. Samples were then centrifuged at 4,000 rpm for 10 minutes to remove debris and precipitated proteins. Approximately 150 µL of supernatant was subsequently transferred to a new 96 well microplate for LC/MS analysis.

Narrow-window mass extraction LC-MS analysis was performed for all samples in this study using a Waters Xevo quadrupole time-of-flight (QTof) mass spectrometer to determine relative peak areas of test compounds. The percent remaining values were calculated using the following equations:

$$\%\, remaining = \frac{A}{A_0} \times 100$$

Where,

A is area response after incubation

A_0 is area response at initial time point

hERG Inhibition Assay

hERG IC_{50} values were generated by Charles River Laboratories (Cleveland, Ohio, United States). Their protocol is described below:

Compounds were tested against cloned hERG potassium channels expressed in HEK293 cells. Chemicals used in solution preparation were purchased from Sigma-Aldrich (St. Louis, MO) unless otherwise noted and were of ACS reagent grade purity or higher. Stock solutions of test articles and the positive control were prepared in dimethyl sulfoxide (DMSO) and stored frozen.

Reference compound concentrations were prepared fresh daily by diluting stock solutions into a Charles River proprietary HEPES-buffered physiological saline (HB-PS) solution which was prepared weekly and refrigerated until use. Since previous results have shown that ≤ 0.3% DMSO did not affect channels currents, all test and control solutions contained 0.3% DMSO. Each test article formulation was sonicated (Model 2510/5510, Branson Ultrasonics, Danbury, CT), at ambient room temperature for 20 minutes to facilitate dissolution. Cells were cultured in Dulbecco's Modified Eagle Medium/Nutrient Mixture F-12 (D-MEM/F-12) supplemented with 10% fetal bovine serum, 100 U/mL penicillin G sodium, 100 µg/mL streptomycin sulfate and 500 µg/mL G418. Before testing, cells in culture dishes were washed twice with Hank's Balanced Salt Solution, detached with accutase. Immediately before use in the IonWorks Barracuda™ system, the cells were washed twice in HB-PS to remove the accutase and re-suspended in 5 mL of HB-PS. The test article effects were evaluated using IonWorks™ Barracuda systems (Molecular Devices Corporation, Union City, CA). HEPES-buffered intracellular solution (Charles River proprietary) for whole cell recordings was loaded into the intracellular compartment of the Population Patch Clamp™ (PPC) planar electrode. Extracellular buffer (HB-PS) was loaded into PPC planar electrode plate wells (11 µL per well). The cell suspension was pipetted into the wells of the PPC planar electrode (9 µL per well). After establishment of a whole-cell configuration (the perforated patch), membrane currents were recorded using patch clamp amplifier in the IonWorks™ Barracuda system. The current recordings were performed one (1) time before test article application to the cells (baseline) and one (1) time after application of the test article. Test article concentrations were applied to naïve cells (n = 4, where n = replicates/ concentration). Each application consisted of addition of 20 µL of 2X concentrated test article solution to the total 40 µL of final volume of the extracellular well of the PPC plate. Duration of exposure to each

compound concentration was five (5) minutes. hERG current was measured using a pulse pattern with fixed amplitudes (conditioning pre-pulse: -80 mV for 25 ms; test pulse: +40 mV for 80 ms) from a holding potential of 0 mV ('zero holding' procedure). hERG current was measured as a difference between the peak current at 1 ms after the test step to +40 mV and the steady-state current at the end of the step to +40 mV.

CYP Inhibition Assay

CYP IC_{50} values were generated by Pharmaron. Their protocol is described below:

1 µL of multiple concentrations of test compound or positive control compound (CYP1A2: furafylline, CYP2B6: ketoconazole, CYP2C8: quercetin, CYP2C9: sulfaphenazole, CYP2C19: N-3-benzylnirvanol, CYP2D6: quinidine and CYP3A4: ketoconazole) was transferred to the "Compound Plate". The concentrations of test compounds and positive control compounds were 0, 0.2, 1, 2, 10, 50, 200, 2000 & 10000 µM. The master solution was prepared with $MgCl_2$ solution (20 µL of 50 mM solution), phosphate buffer (100 µL of 200 mM solution), ultra-pure water (56 µL), human liver microsomes (2 µL of 20 mg/mL stock concentration (Corning® UltraPool™ HLM 150, Mixed Gender Cat. No.: 452117)) and 1 µL of substrate (CYP1A2: phenacetin (8 mM stock concentration), CYP2B6: bupropion (10 mM stock concentration), CYP2C8: paclitaxel (1 mM stock concentration), CYP2C9: tolbutamide (40 mM stock concentration), CYP2C19: mephenytoin (10 mM stock concentration), CYP2D6: dextromethorphan (2 mM stock concentration) and CYP3A4: midazolam (1 mM stock concentration) and testosterone (10 mM stock concentration). The master solution was pre-warmed in a water bath at 37 °C for 5 minutes. 179 µL of the incubated-master solution was transferred to the compound plate. In the mixed system, the final concentrations of test compounds and positive control compounds were 0, 0.001,

0.005, 0.01, 0.05, 0.25, 1, 10 & 50 uM. All experiments were performed in duplicate. The reaction was started with the addition of 20 μL of 10 mM NADPH solution at the final concentration of 1 mM. The reaction was stopped by the addition of 1.5 volumes of methanol with IS (100 nM alprazolam, 200 nM imipramine, 200 nM labetalol and 2 μM ketoprofen) to the "Incubation Plate" at the designated time points (20 minutes for CYP1A2, 2B6, 2C9, 2C19 and 2D6, 5 minutes for midazolam mediated 3A4, 10 minutes for testosterone mediated 3A4). The "Incubation Plate" was centrifuged at 3,220 g for 40 minutes to precipitate protein. Aliquot of 100 μL of the supernatant was diluted by 100 μL ultra-pure H_2O, and the mixture was used for LC-MS/MS analysis. The formation of metabolites was analyzed by using LC-MS/MS. A decrease in the formation of the metabolites in peak area to vehicle control was used to calculate an IC_{50} value (test compound concentration which produces 50% inhibition) by using Excel XLfit.

***In Vivo* Pharmacokinetic Studies**

The pharmacokinetic profiles of **8b**, **26a** and **26b** were assessed by Pharmaron. Their protocol is described below:

Test compounds were dissolved first in DMSO, then mixed with 47.5% PEG400 and 47.5% DI water with 10% Tween80. The solutions were thoroughly vortexed after each step and stored at room temperature. Solutions were freshly prepared on the day of dosing. Female CB17 SCID mice (n = 3) (6-8 weeks old, 17-20 g weight) were orally administered a 10 mg/kg dose (10 mL/kg dose volume, 1 mg/mL concentration) of the test compound. Blood samples were taken via the dorsal metatarsal vein at 0.25, 0.5, 1, 2, 4, 8, and 24 h post-dose. Blood samples were transferred into plastic microcentrifuge tubes containing the anticoagulant Heparin-Na and centrifuged at

4000g for 5 minutes at 4°C to obtain plasma. The samples were stored in a freezer at -75±15° C prior to analysis.

To determine brain concentrations, female CB17 SCID mice (*n* = 3) (6-8 weeks old, 17-20 g weight) were orally administered a 100 mg/kg dose (10 mL/kg dose volume, 10 mg/mL concentration) of the test compound. 4 hours post-dose, the animals were terminally anaesthetized by a rising concentration of CO_2. Their chest cavities were opened to expose the heart and an incision at the right auricle by surgical scissors was done. A syringe full of gentle saline was pushed into the heart slowly via left ventricle (saline volume: ~ 10 mL). The animal was placed head down at a 45° angle to facilitate blood removal. Brain samples were collected and kept frozen at -75±15° C. All brain samples were weighed and homogenized with phosphate buffered saline (PBS) by brain weight (g) to buffer volume (mL) ratio 1:3 before analysis. The actual concentrations were the detected value multiplied by the dilution factor.

Concentrations of the test compound in the plasma samples were analyzed using a LC-MS/MS method. WinNonlin (Phoenix^{TM}, version 8.0) or other similar software was used for pharmacokinetic calculations. The following pharmacokinetic parameters were calculated, whenever possible from the plasma concentration versus time data:

PO administration: $T_{1/2}$, C_{max}, T_{max}, AUC_{last}, AUC_{inf} and F.

All animal procedures were in accordance with the regulations of Institutional Animal Care and Use Committee (IACUC) at Pharmaron Inc.

Co-Crystallization of ALK2 with M4K2149

Protein expression and purification:

Constructs were prepared by ligation-independent cloning. The kinase domain of ALK2 (residues 201–499; Uniprot ID, Q04771) was cloned into pFB-LIC-Bse for baculoviral expression. The construct was verified by sequencing. ALK2 was expressed in Sf9 insect cells grown at 27 °C. Some 72 h post-infection, cells were harvested and lysed using ultrasonication. ALK2 was initially purified by nickel affinity chromatography before subsequent purification by size exclusion chromatography (Superdex 200 16/600). The eluted protein was stored in 50 mM HEPES, pH 7.5, 300 mM NaCl, 10 mM DTT. The hexahistidine tag of ALK2 was cleaved using tobacco etch virus protease after initial nickel purification.

Crystallization

Crystallization was achieved at 4 °C using the sitting-drop vapor diffusion method. ALK2 was preincubated with 1 mM M4K2149 at a protein concentration of 11 mg/mL and crystallized using a precipitant containing 0.1 M citrate pH 4.9, 1 M ammonium sulfate and 0.2 M sodium/potassium tartrate. Viable crystals were obtained when the protein solution was mixed with the reservoir solution at 2:1 volume ratio. Crystals were cryoprotected with mother liquor plus 25% ethylene glycol, prior to vitrification in liquid nitrogen.

Data Collection

Diffraction data were collected at the Diamond Light Source, station I03 using monochromatic radiation at wavelength 0.9763 Å.

Phasing, Model Building, Refinement, and Validation

Data were processed with Xia2 and subsequently scaled using the program AIMLESS from the CCP4 suite.[40-41] Initial phases were obtained by molecular replacement using the program PHASER and the structure of ALK2 (Protein Data Bank code 6SRH) as a search model.[42] The resulting structure solution was refined using Phenix Refine and manually rebuilt with COOT.[43-

[44] The complete structure was verified for geometric correctness with MolProbity.[45] Data collection and refinement statistics can be found in Supplemental Table 1.

Co-crystal images in the article were processed using Molsoft MolBrowser 3.8.

ASSOCIATED CONTENT

Supporting Information

The Supporting Information is available free of charge.

^{1}H and ^{19}F NMR spectra of select compounds, crystallization methods, Caco-2 and HLM & MLM data, CYP and hERG inhibition data, kinase selectivity panel.

Accession Codes

PBD ID codes: ALK2-**M4K2149**, 6T6D; ALK2-**LDN-213844**, 4BGG.

Authors will release the atomic coordinates and experimental data upon article publication.

AUTHOR INFORMATION

Corresponding Author

*Phone: +1 (416) 673-8577; E-mail: Rima.Alawar@oicr.on.ca

Present Addresses

‡ Dalriada Therapeutics Inc., 3252 Respond Road, Mississauga, Ontario L5M 7X4, Canada

Author Contributions

Analogs were synthesized by D.E., D.S. and D.P. The compounds were designed and their syntheses devised by D.S., M.I., C.A.Z.-V. and D.E. All NanoBRET data was generated by J. F. W. Crystallography experiments were performed by E.W. and R.A. Caco-2 and microsomal stability studies were conducted by T.K. HRMS were also generated by T.K. A.N.B., A.A., J.O., M.I. and R.Al. were involved in experimental design, the interpretation of data and monitored project progress. O.G.R. and A.M.E. initiated the project and edited the paper. The manuscript was written by D.E. and revised by D.S., C.A.Z.-V., M.I. and R.Al.

Notes

The authors declare no competing financial interest.

ACKNOWLEDGMENT

This work was funded by the Cancer Therapeutics Innovation Pipeline program at the Ontario Institute for Cancer Research (OICR). The OICR receives financial support from the Government of Ontario through the Ministry of Training, Colleges and Universities. Funding from The Brain Tumour Charity was used to support the cellular and crystallographic research conducted at the University of Oxford. The SGC is a registered charity (number 1097737) that receives funds from AbbVie, Bayer Pharma AG, Boehringer Ingelheim, Canada Foundation for Innovation, Eshelman Institute for Innovation, Genome Canada through Ontario Genomics Institute [OGI-055], Innovative Medicines Initiative (EU/EFPIA) [ULTRA-DD grant no. 115766], Janssen, Merck KGaA, Darmstadt, Germany, MSD, Novartis Pharma AG, Pfizer, São Paulo Research Foundation-FAPESP, Takeda, and Wellcome [106169/ZZ14/Z]. We thank Reaction Biology Corporation for their *pro bono* contributions in testing the biological activity of our compounds. D.P. is grateful to NSERC for the Collaborative Research and Training

Experience 432008-2013 grant. We would like to thank Dr. Gennady Poda for generating the Oracle database where compound data was stored and for providing his expertise on molecular modeling. We would also like to thank Mehakpreet Saini for contributing to the writing and editing of ADME protocols.

ABBREVIATIONS

ALK2, activin receptor-like kinase-2; ALK5, activin receptor-like kinase-5; ATP, adenosine triphosphate; AUC_{inf}, area under the curve (extrapolated to infinity); BBB, blood-brain barrier; BMP, bone morphogenetic protein; B/P, total brain-to-plasma ratio; $C_{b,u}$, unbound brain concentration; cLogP, calculated lipophilicity; C_{max}, maximum concentration; CNS, central nervous system; DIPG, diffuse intrinsic pontine glioma; EDC, 1-ethyl-3-(3-dimethylaminopropyl)carbodiimide; FOP, fibrodysplasia ossificans progressiva; GS, glycine-serine rich domain; HATU, hexafluorophosphate azabenzotriazole tetramethyl uronium; HBD, hydrogen bond donor; HDACi, histone deacetylase inhibitors; hERG, human ether a-go-go related gene; HLM, human liver microsome; MLM, mouse liver microsome; PK, pharmacokinetic; P-gp, P-glycoprotein; SAR, structure-activity relationship; STKR, serine/threonine kinase receptor; TFA, trifluoroacetic acid; TGFβ-R1, transforming growth beta receptor 1; tPSA, total polar surface area; WT, wild-type.

REFERENCES

1. Heffron, T. P. Small molecule kinase inhibitors for the treatment of brain cancer. *J. Med. Chem.* **2016**, *59*, 10030-10066.

2. Di, L.; Rong, H.; Feng, B. Demystifying brain penetration in central nervous system drug discovery. *J. Med. Chem.* **2013**, *56*, 2-12.

3. Pacifici, M.; Shore, E. M. Common mutations in ALK2/ACVR1, a multi-faceted receptor, have roles in distinct pediatric musculoskeletal and neural orphan disorders. *Cytokine Growth Factor Rev.* **2016**, *27*, 93-104.

4. Schmierer, B.; Hill, C. S. TGFβ-SMAD signal transduction: molecular specificity and functional flexibility. *Nat. Rev. Mol. Cell Biol.* **2007**, *8*, 970-982.

5. Massagué, J.; Blain, S. W.; Lo, R. S. TGFβ signaling in growth control, cancer, and heritable disorders. *Cell* **2000**, *103*, 295-309.

6. Taylor, K. R.; Vinci, M.; Bullock, A. N.; Jones, C. *ACVR1* mutations in DIPG: lessons learned from FOP. *Cancer Res.* **2014**, *74*, 4565-4570.

7. Taylor, K. R.; Mackay, A.; Truffaux, N.; Butterfield, Y. S.; Morozova, O.; Philippe, C.; Castel, D.; Grasso, C. S.; Vinci, M.; Carvalho, D.; Carcaboso, A. M.; de Torres, C.; Cruz, O.; Mora, J.; Entz-Werle, N.; Ingram, W. J.; Monje, M.; Hargrave, D.; Bullock, A. N.; Puget, S.; Yip, S.; Jones, C.; Grill, J. Recurrent activating *ACVR1* mutations in diffuse intrinsic pontine glioma. *Nat. Genet.* **2014**, *46*, 457-461.

8. Mathew, R. K.; Rutka, J. T. Diffuse intrinsic pontine glioma: clinical features, molecular genetics, and novel targeted therapeutics. *J. Korean Neurosurg. Soc.* **2018**, *61*, 343-351.

9. Warren, K. E. Diffuse intrinsic pontine glioma: poised for progress. *Front. Oncol*. **2012**, *2*, 205.

10. Wu, G.; Diaz, A. K.; Paugh, B. S.; Rankin, S. L.; Ju, B.; Li, Y.; Zhu, X.; Qu, C.; Chen, X.; Zhang, J.; Easton, J.; Edmonson, M.; Ma, X.; Lu, C.; Nagahawatte, P.; Hedlund, E.; Rusch, M.; Pounds, S.; Lin, T.; Onar-Thomas, A.; Huether, R.; Kriwacki, R.; Parker, M.; Gupta, P.; Becksfort, J.; Wei, L.; Mulder, H. L.; Boggs, K.; Vadodaria, B.; Yergeau, D.; Russell, J. C.; Ochoa, K.; Fulton, R. S.; Fulton, L. L.; Jones, C.; Boop, F. A.; Broniscer, A.; Wetmore, C.; Gajjar, A.; Ding, L.; Mardis, E. R.; Wilson, R. K.; Taylor, M. R.; Downing, J. R.; Ellison, D. W.; Zhang, J.; Baker, S. J. The genomic landscape of diffuse intrinsic pontine glioma and pediatric non-brainstem high-grade glioma. *Nat. Genet.* **2014**, *46*, 444-450.

11. Carvalho, D.; Taylor, K. R.; Olaciregui, N. G.; Molinari, V.; Clarke, M.; Mackay, A.; Ruddle, R.; Henley, A.; Valenti, M.; Hayes, A.; Brandon, A. D. H.; Eccles, S. A.; Raynaud, F.; Boudhar, A.; Monje, M.; Popov, S.; Moore, A. S.; Mora, J.; Cruz, O.; Vinci, M.; Brennan, P. E.; Bullock, A. N.; Carcaboso, A. M.; Jones, C. ALK2 inhibitors display beneficial effects in preclinical models of *ACVR1* mutant diffuse intrinsic pontine glioma. *Commun. Biol.* **2019**, *2*, 156.

12. Anastas, J. N.; Zee, B. M.; Kalin, J. H.; Kim, M.; Guo, R.; Alexandrescu, S.; Blanco, M. A.; Giera, S.; Gillespie, S. M.; Das, J.; Wu, M.; Nocco, S.; Bonal, D. M.; Nguyen, Q.-D.; Suva, M. L.; Bernstein, B. E.; Alani, R.; Golub, T. R.; Cole, P. A.; Filbin, M. G.; Shi, Y. Re-programing chromatin with a bifunctional LSD1/HDAC inhibitor induces therapeutic differentiation in DIPG. *Cancer Cell*, **2019**, *36*, 528-544.

13. Hopkins, C. R. Inhibitors of the bone morphogenetic protein (BMP) signaling pathway: a patent review (2008-2015). *Expert Opin. Ther. Pat.* **2016**, *26*, 1115-1128.

14. Cuny, G. D.; Yu, P. B.; Laha, J. K.; Xing, X.; Liu, J.-F.; Lai, C. S.; Deng, D. Y.; Sachidanandan, C.; Bloch, K. D.; Peterson, R. T. Structure-activity relationship study of bone morphogenetic protein (BMP) signaling inhibitors. *Bioorg. Med. Chem. Lett.* **2008**, *18*, 4388-4392.

15. Yu, P. B.; Cuny, G. D.; Mohedas, A. H.; Bloch, K. D.; Peterson, R. T. BMP inhibitors and methods of use thereof. WO 2014/138088 A1, 2014.

16. Sanvitale, C. E.; Kerr, G.; Chaikuad, A.; Ramel, M.-C.; Mohedas, A. H.; Reichert, S.; Wang, Y.; Triffitt, J. T.; Cuny, G. D.; Yu, P. B.; Hill, C. S.; Bullock, A. N. A new class of small molecule inhibitor of BMP signaling. *PLoS One* **2013**, *8*, e62721.

17. Mohedas, A. H.; Wang, Y.; Sanvitale, C. E.; Canning, P.; Choi, S.; Xing, X.; Bullock, A. N.; Cuny, G. D.; Yu, P. B. Structure-activity relationship of 3,5-diaryl-2-aminopyridine ALK2 inhibitors reveals unaltered binding affinity for fibrodysplasia ossificans progressiva causing mutants. *J. Med. Chem.* **2014**, *57*, 7900-7915.

18. Yu, P. B.; Cuny, G. D.; Mohedas, A. H. Compositions and methods for inhibiting BMP. WO 2015/148654 A1, 2015.

19. Reinecke, M.; Ruprecht, B.; Poser, S.; Wiechmann, S.; Wilhelm, M.; Heinzlmeir, S.; Kuster, B.; Médard, G. Chemoproteomic selectivity profiling of PIKK and PI3K kinase inhibitors. *ACS Chem. Biol.* **2019**, *14*, 655-664.

20. Herbertz, S.; Sawyer, J. S.; Stauber, A. J.; Gueorguieva, I.; Driscoll, K. E.; Estrem, S. T.; Cleverly, A. L.; Desaiah, D.; Guba, S. C.; Benhadji, K. A.; Slapak, C. A.; Lahn, M. M. Clinical development of galunisertib (LY2157299 monohydrate), a small molecule

inhibitor of transforming growth factor-beta signaling pathway. *Drug Des., Dev. Ther.* **2015**, *9*, 4479-4499.

21. Unpublished results. Data can be viewed in presentations archived at https://m4kpharma.com/blog/.

22. Morgan, M. R.; Roberts, O. G.; Edwards, A. M. Ideation and implementation of an open science drug discovery business model - M4K Pharma. *Wellcome Open Res*. **2018**, *3*, 154.

23. Chaikuad, A.; Alfano, I.; Kerr, G.; Sanvitale, C. E.; Boergermann, J. H.; Triffitt, J. T.; von Delft, F.; Knapp, S.; Knaus, P.; Bullock, A. N. Structure of the bone morphogenetic protein receptor ALK2 and implications for fibrodysplasia ossificans progressiva. *J. Biol. Chem.* **2012**, *287*, 36990-36998.

24. Rankovic, Z. CNS drug design: balancing physicochemical properties for optimal brain exposure. *J. Med. Chem.* **2015**, *58*, 2584-2608.

25. tPSA, pKa and cLogP values were calculated using ChemDraw Professional 19.0.

26. Johnson, T. W.; Richardson, P. F.; Bailey, S.; Brooun, A.; Burke, B. J.; Collins, M. R.; Cui, J. J.; Deal, J. G.; Deng, Y.-L.; Dinh, D.; Engstrom, L. D.; He, M.; Hoffman, J.; Hoffman, R. L.; Huang, Q.; Kania, R. S.; Kath, J. C.; Lam, H.; Lam, J. L.; Le, P. T.; Lingardo, L.; Liu, W.; McTigue, M.; Palmer, C. L.; Sach, N. W.; Smeal, T.; Smith, G. L.; Stewart, A. E.; Timofeevski, S.; Zhu, H.; Zhu, J.; Zou, H. Y.; Edwards, M. P. Discovery of (10*R*)-7-amino-12-fluoro-2,10,16-trimethyl-15-oxo-10,15,16,17-tetrahydro-*2H*-8,4-(metheno)pyrazolo[4,3-*h*][2,5,11]-benzoxadiazacyclotetradecine-3-carbonitrile (PF-06463922), a macrocyclic inhibitor of anaplastic lymphoma kinase (ALK) and c-ros

oncogene 1 (ROS1) with preclinical brain exposure and broad-spectrum potency against ALK-resistant mutations. *J. Med. Chem.* **2014**, *57*, 4720-4744.

27. Kuhn, B.; Mohr, P.; Stahl, M. Intramolecular hydrogen bonding in medicinal chemistry. *J. Med. Chem.* **2010**, *53*, 2601-2611.

28. Gillis, E. P.; Eastman, K. J.; Hill, M. D.; Donnelly, D. J.; Meanwell, N. A. Applications of fluorine in medicinal chemistry. *J. Med. Chem*. **2015**, *58*, 8315-8359.

29. Johnson, T. W.; Gallego, R. A.; Edwards, M. P. Lipophilic efficiency as an important metric in drug design. *J. Med. Chem.* **2018**, *61*, 6401-6420.

30. Sekimata, K.; Sato, T.; Sakai, N.; Watanabe, H.; Mishima-Tsumagari, C.; Taguri, T.; Matsumoto, T.; Fujii, Y.; Handa, N.; Honma, T.; Tanaka, A.; Shirouzu, M.; Yokoyama, S.; Miyazono, K.; Hashizume, Y.; Koyama, H. Bis-heteroaryl pyrazoles: identification of orally bioavailable inhibitors of activin receptor-like kinase-2 (R206H). *Chem. Pharm. Bull.* **2019**, *67*, 224-235.

31. Khalili, F.; Henni, A.; East, A. L. L. pK_a values of some piperazines at (298, 303, 313, and 323) K. *J. Chem. Eng. Data* **2009**, *54*, 2914-2917.

32. Jiang, J.-k.; Huang, X.; Shamim, K.; Patel, P. R.; Lee, A.; Wang, A. Q.; Nguyen, K.; Tawa, G.; Cuny, G. D.; Yu, P. B.; Zheng, W.; Xu, X.; Sanderson, P.; Huang, W. Discovery of 3-(4-sulfamoylnaphthyl)pyrazolo[1,5-*a*]pyrimidines as potent and selective ALK2 inhibitors. *Bioorg. Med. Chem. Lett.* **2018**, *28*, 3356-3362.

33. Chen, J.; Ding, C. Z.; Dragovich, P.; Fauber, B.; Gao, Z.; Labadie, S.; Lai, K. W.; Purkey, H. E.; Robarge, K.; Wei, B.; Zhou, A. Piperidine-dione derivatives. WO 2015/140133 A1, 2015.

34. Mascitti, V.; McClure, K. F.; Munchhof, M. J.; Robinson, R. P., Jr. 4-(5-cyano-pyrazol-1-yl)-piperidine derivatives as GPR 119 modulators. WO 2012/069948 A1, 2012.

35. Zhan, W.; Ji, L.; Ge, Z.-m.; Wang, X.; Li, R.-t. A continuous-flow synthesis of primary amides from hydrolysis of nitriles using hydrogen peroxide as oxidant. *Tetrahedron* **2018**, *74*, 1527-1532.

36. Whitehead, A.; Ornoski, O.; Raghavan, S.; Berger, R.; Garfunkle, J.; Yang, Z.; Ji, G.; Jiang, F.; Fu, J. Fused pyrazine derivatives useful as soluble guanylate cyclase stimulators. WO 2017/200825 A1, 2017.

37. Balkovec, J. M.; Bensen, D. C.; Borchardt, A.; Brady, T. P.; Chen, Z.; Lam, T.; Tari, L. W. Small molecule inhibitors of dihydrofolate reductase. WO 2016/201219 A1, 2016.

38. Pouzet, P.; Hoenke, C.; Nickolaus, P.; Goeggel, R.; Fox, T.; Fiegen, D.; Klinder, K. Novel piperazino-dihydrothienopyrimidine derivatives. WO 2009/050236 A1, 2009.

39. Guerin, D. J.; Bair, K. W.; Caravella, J. A.; Ioannidis, S.; Lancia Jr.; D. R.; Li, H.; Mischke, S.; Ng, P. Y.; Richard, D.; Schiller, S. E. R.; Shelekhin, T.; Wang, Z. Thienopyridine carboxamides as ubiquitin-specific protease inhibitors. WO 2017/139778 A1, 2017.

40. Winter, G. xiz2: an expert system for macromolecular crystallography data reduction. *J. Appl. Crystallogr.* **2010**, *43*, 186-190.

41. Winn, M. D.; Ballard, C. C.; Cowtan, K. D.; Dodson, E. J.; Emsley, P.; Evans, P. R.; Keegan, R. M.; Krissinel, E. B.; Leslie, A. G. W.; McCoy, A.; McNicholas, S. J.; Murshudov, G. N.; Pannu, N. S.; Potterton, E. A.; Powell, H. R.; Read, R. J.; Vagin, A.; Wilson, K. S. Overview of the CCP4 suite and current developments. *Acta Crystallogr., Sect. D: Biol. Crystallogr.* **2011**, *D67*, 235-242.

42. McCoy, A. J.; Grosse-Kunstleve, R. W.; Adams, P. D.; Winn, M. D.; Storoni, L .C.; Read, R. J. Phaser crystallographic software. *J. Appl. Crystallogr.* **2007**, *40*, 658-674.

43. Adams, P. D.; Afonine, P.V.; Bunkóczi, G.; Chen, V. B.; Davis, I. W.; Echols, N.; Headd, J. J.; Hung, L.-W.; Kapral, G. J.; Grosse-Kunstleve, R. W.; McCoy, A. J.; Moriarty, N. W.; Oeffner, R.; Read, R. J.; Richardson, D. C.; Richardson, J. S.; Terwilliger, T. C.; Zwart, P. H. PHENIX: a comprehensive Python-based system for macromolecular structure solution. *Acta Crystallogr., Sect. D: Biol. Crystallogr.* **2010**, *D66*, 213-221.

44. Emsley, P.; Cowtan, K. Coot: model-building tools for molecular graphics. *Acta Crystallogr., Sect. D: Biol. Crystallogr.* **2004**, *D60*, 2126-2132.

45. Davis, I. W.; Leaver-Fay, A.; Chen, V. B.; Block, J. N.; Kapral, G. J.; Wang, X.; Murray, L. W.; Arendall III, W. B.; Snoeyink, J.; Richardson, J. S.; Richardson, D. C. MolProbity: all-atom contacts and structure validation for proteins and nucleic acids. *Nucleic Acids Res.* **2007**, *35*, 375-383.

For Table of Contents Only

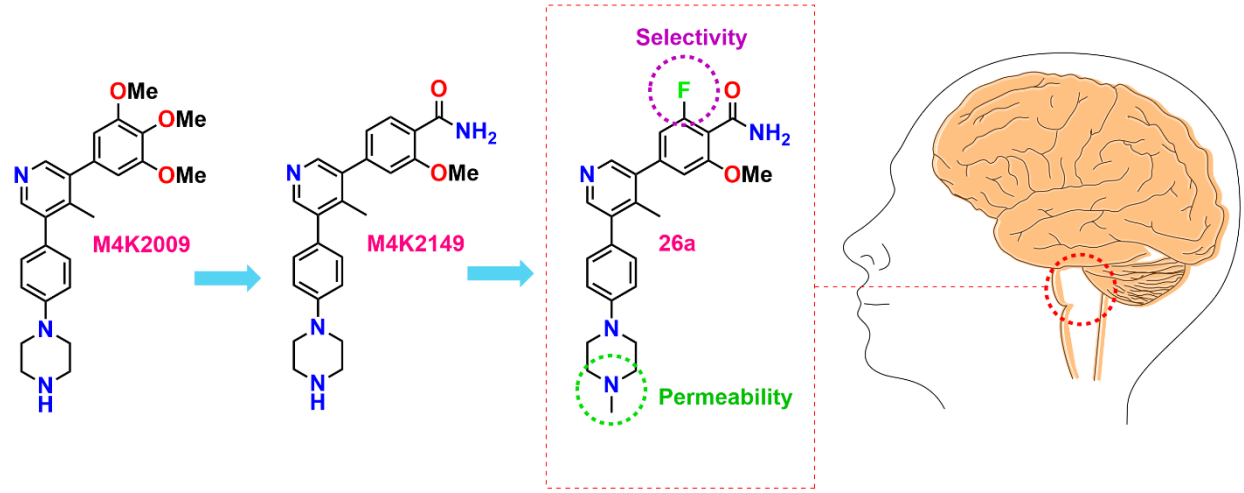

ALK2 IC_{50} = 13 nM
ALK5/ALK2 = 141
hERG IC_{50} = 8 μM
Caco-2 Efflux = 1.8

ALK2 IC_{50} = 17 nM
ALK5/ALK2 = 34
hERG IC_{50} = >30 μM
Caco-2 Efflux = 8.1

ALK2 IC_{50} = 3 nM
ALK5/ALK2 = 350
hERG IC_{50} = >30 μM
Caco-2 Efflux = 2.9

Developing therapies for childhood brain cancer